Drosophila Activin signaling promotes muscle growth through InR/dTORC1 dependent and independent processes.

Myung-Jun Kim[1] and Michael B. O'Connor[1*]

[1]Department of Genetics, Cell Biology and Development

University of Minnesota

Minneapolis, MN 55455

*Corresponding author
Michael B. O'Connor
University of Minnesota
Department of Genetics, Cell Biology and Development
6-160 Jackson Hall
321 Church St. SE
612-626-0642

Summary

The Myostatin/Activin branch of the TGFβ superfamily acts as a negative regulator of mammalian skeletal muscle size, in part, through downregulation of insulin/IGF-1 signaling. Surprisingly, recent studies in *Drosophila* indicate that Activin signaling acts as a positive regulator of muscle size. In this study, we demonstrate that *Drosophila* Activin signaling positively regulates the InR/dTORC1 pathway and the level of MHC, an essential sarcomeric protein, via promoting the transcription of *Pdk1* and *Akt1*. Enhancing InR/dTORC1 signaling in the muscle of Activin pathway mutants restores MHC levels close to wild-type, but only increased the width of muscle cells. In contrast, hyperactivation of the Activin pathway increases the length of muscle cells even when MHC levels were lowered by suppression of dTORC1. Together, these results indicate that *Drosophila* Activin pathway regulates larval muscle geometry via promoting InR/dTORC1-dependent MHC production and the differential assembly of sarcomeric components into either pre-existing (width) or new (length) sarcomeric units depending on the balance of InR/dTORC1 and Activin signals.

Introduction

Skeletal muscle accounts for a large portion of the body mass in various species including mammals (Gunn, 1989) and flying insects (Marden, 2000). It is essential not only for mobility but also for organismal energy balance and metabolism as it is a primary tissue for insulin-stimulated glucose consumption [reviewed in (Stump, et al., 2006)]. Skeletal muscle is also proposed to be an endocrine organ that secretes a plethora of bioactive molecules, known as myokines, many of which depend on muscle contraction for production and secretion. Current evidence suggests that myokines exert substantial influence on the physiology and activity of their various target tissues [reviewed in (Pedersen and Febbraio, 2012)]. Therefore, achieving and maintaining an appropriate skeletal muscle mass and cellular function is likely to be essential for good health and quality of life.

Accordingly, multiple signaling pathways are known to act in concert to achieve and maintain proper muscle mass [reviewed in (Piccirillo, et al., 2014; Schiaffino, et al., 2013)]. Among these, Myostatin (Mstn), a member of the TGF-β superfamily of growth and differentiation factors, has proven to be a prominent player. Loss-of-function mutations in *mstn* have been identified or induced in a large variety of mammals including mice, cattle, dogs, sheep and humans (Mosher, et al., 2007; Clop, et al., 2006; Schuelke, et al., 2004; Kambadur, et al., 1997; McPherron, et al., 1997; McPherron and Lee, 1997). In all these species, loss of *mstn* results in larger skeletal muscles leading to the conclusion that Mstn is a negative regulator of muscle mass. Mechanistically, the increase in skeletal muscle mass caused by disruption of the *mstn* gene has been attributed to excess proliferation of muscle progenitors (hyperplasia) that is manifested by a larger number of fibers, as well as to hypertrophy of each muscle fiber causing bigger cross-

sectional area (Amthor, et al., 2009; McPherron, et al., 1997). However, several more recent studies suggest that the hypertrophy of individual muscle fibers may be the predominant mechanism to increase the muscle mass, with a minimal contribution from hyperplasia (Lee, et al., 2012; Amthor, et al., 2009; Sartori, et al., 2009). In addition, satellite cells (muscle stem cells) do not appear to contribute to the muscle hypertrophy (Amthor, et al., 2009; Sartori, et al., 2009). Taken together, these results indicate that the hypertrophy of individual myofibers rather than increases in myofiber and myonuclei number is the chief mechanism for enhanced muscle growth in *mstn* mutants.

In addition to Mstn, Activins, additional members in TGF-β/Activin signaling branch, have also been shown to negatively affect the muscle mass (Chen, et al., 2017; Chen, et al., 2014). The Mstn and Activins appear to synergize in suppressing muscle growth since co-inhibition of both factors resulted in a greater increases in muscle mass than those in which the activity of individual factors was inhibited (Chen, et al., 2017). Finally, expression of a dominant negative form of ActRIIB, a high affinity activin type 2 receptor for Mstn , Activins and several other ligands in the TGF-β/Activin subfamily (Souza, et al., 2008; Lee and McPherron, 2001), leads to muscle hypertrophy (Lee and McPherron, 2001), suggesting an important role for ActRIIB in relaying the negative effect of Mstn and Activins on muscle growth.

Consistent with the idea that Mstn and Activins are negative regulators of muscle growth, overexpression of these factors has been shown to promote the loss of muscle weight both in rats (Amirouche, et al., 2009) and mice (Chen, et al., 2014; Zimmers, et al., 2002). This is analogous to what happens during muscle disuse (Gustafsson, et al., 2010; Reardon, et al., 2001; Wehling, et al., 2000) and cancer cachexia (Loumaye, et al., 2015; Marino, et al., 2015; Lokireddy, et al., 2012), in which muscle wasting correlates with the increased expression of Mstn or Activins.

Interestingly, cancer cachexia was reversed by prodomain-derived ligand-specific antagonists (Chen, et al., 2017) or by a decoy receptor of ActRIIB (Zhou, et al., 2010). Besides reversing the cancer cachexia, inhibition of Mstn or Activins is also known to alleviate the atrophy and malfunctioning of dystrophic muscle (Chen, et al., 2017; Bogdanovich, et al., 2002). Therefore, Mstn- and Activin-induced signaling pathways appear to play essential roles in the development of pathogenic muscle wasting associated with cancer, dystrophy, and perhaps age related sarcopenia (Bergen, et al., 2015; White and LeBrasseur, 2014) and may provide potent therapeutic targets for the treatment of muscle atrophy in multiple settings.

Although the vast majority of data strongly supports a negative role of Mstn/Activin signaling on muscle growth, there are some conflicting reports when manipulation of pathway activity is done at the R-Smad level. For example, inhibition of Smad2 and 3, the two R-Smads devoted to TGF-β/Activin subfamily signaling, in adults through shRNA transfection led to an increase in cross-sectional area of the muscle fibers (Sartori, et al., 2009) consistent with these Smads acting to inhibit muscle fiber growth. However Smad3 knockout mice actually exhibit smaller bodies and a ~10% reduction in the muscle fiber size (Tan, et al., 2011). Furthermore depletion of Smad2 as well as double deficiency of Smad2 and 3 in a mouse muscle injury model did not appear to increase the muscle fiber size (Tando, et al., 2016) as would be expected if the Mstn and Activin pathways signaled primary in a canonical manner through the R-Smads to negatively regulate muscle growth. These results suggest that Mstn/Activin regulation of muscle mass may be more complicated than is presently assumed.

A well-documented consequence of Mstn and Activin-induced signaling in the skeletal muscle is the inhibition of IGF-1/PI3K/AKT pathway. Specifically, overexpression of *mstn* via *in vivo* transfection in the adult muscle leads to attenuated phosphorylation of AKT, S6 and 4E-BP

(Amirouche, et al., 2009). Conversely, inhibition of Mstn and Activin by prodomain-derived antagonists leads to increased phosphorylation of mTOR and S6RP (Chen, et al., 2017). In addition, administration of a soluble decoy receptor of ActRIIB to adult mice resulted in increased phosphorylation of AKT and FOXO3a in skeletal muscle (Zhou, et al., 2010). These are all consistent with the idea that Mstn or Activin-induced signals lead to inhibition of the IGF-1/AKT/mTOR function. Finally, the inhibitory effect of Mstn on IGF-1/AKT/mTOR signaling was reproduced in human myoblast cultures where addition of these factors decreased phosphorylation of AKT, FOXO1 and p70S6K (Lokireddy, et al., 2011; Trendelenburg, et al., 2009). Since the IGF-1/AKT/mTOR pathway is the most important anabolic stimulus for muscle growth (Egerman and Glass, 2014), much of the influence of Mstn and Activins on muscle mass is likely attributed to the inhibition of IGF-1/AKT/mTOR pathway.

Drosophila skeletal muscles exhibit tremendous (around 50-fold) growth during larval stages (Piccirillo, et al., 2014). This growth occurs through an increase in individual cell size without contribution from muscle stem cells (Piccirillo, et al., 2014; Demontis and Perrimon, 2009). This process is mechanistically similar to mammalian muscle hypertrophy shown by *mstn* mutants that largely depends on growth of individual myofibers making *Drosophila* a good model for exploring the role of Activin signaling in regulating muscle fiber growth. In addition, the Activin signaling network is significantly simpler in *Drosophila* compared to vertebrates and consists of only three ligands, Activin beta (Actβ), Dawdle (Daw) and Myoglianin (Myo), a close homolog of vertebrate Myostatin, that signal through a single type I receptor, Baboon and a single R-Smad known as dSmad2 or Smox [reviewed in (Parker, et al., 2004)]. Intriguingly, we have recently shown that unlike vertebrates, the *Drosophila* Activin-like ligand Actβ is a positive regulator of larval muscle mass (Moss-Taylor, et al., 2019). To distinguish whether this positive as opposed

to negative growth function is a general feature of the entire Activin signaling network or represents an aberration due to loss of only one ligand, we analyzed muscle growth in *babo* and *dSmad2* null mutants which eliminate signaling of the entire pathway. We find that when the entire Activin signaling pathway is compromised by loss of either *babo* or *dSmad2*, larval muscles are reduced in both length and width similar to what we observe for *Actβ* loss alone. Loss of either *myo* alone or *daw* alone, does not appreciably affect larval muscle size. Hyperactivation of the Activin pathway through expression of constitutively activated Babo produces larger muscles in which length is disproportionally increased relative to width. Mechanistically, we find that loss of *babo* or *dSmad2* leads to attenuated expression of *Pdk1* and *Akt1*, two essential components of Insulin-like receptor (InR) signaling pathway, and decreased production of myosin heavy chain (MHC). Increasing activation of InR/dTORC1 signaling in a *dSmad2* mutant background restores MHC production, but only increases muscle width, whereas expression of activated Babo in a dTORC1 compromised individual increases muscle length even through MHC level is reduced. We infer that Activin signaling differentially controls larval muscle growth in two ways. First, it regulates sarcomeric protein production via positive effects on the InR/dTORC1 pathway, and second it differentially regulates the serial (length) verses lateral (width) addition of sarcomeric units depending on the dose of the Activin signal.

Materials and Methods

Drosophila strains and husbandry

Fly lines were kept on standard cornmeal-yeast-agar medium at 25ₒC. For experiments involving *babo, dSmad2* and *daw* mutants, larvae were raised on yeast paste placed on apple juice-agar plates since the *babo, dSmad2* and *daw* mutants do not grow well on standard medium. The

w^{1118} strain was used as a wild-type (*wt*) control for *babo*, *dSmad2* and ligand mutants. *dSmad2*^{F4}, *babo*^{fd4}, *babo*^{df}, *Actβ*^{ed80}, *daw*^{1}, *daw*^{11}, *myo*^{1}, *UAS-dSmad2* and *UAS-babo*^{CA} (constitutively active) lines have been described previously (Kim and O'Connor, 2014; Ting, et al., 2007; Brummel, et al., 1999). *myo*^{CR2} was generated by BestGene Inc by CRISPR-mediated mutagenesis using 5'-CTTCGACTATTCACCGCGCTATTA-3' as a guide RNA. The resulting line contains a 1 bp deletion resulting in frameshift and stop prior to the ligand domain and is a putative null mutant. (Fig. S1C). The *Mef2-Gal4* (BL27390) line was used as a muscle driver throughout the study except in the RNA-seq analysis. To ensure that the results observed in this study are the consequence of muscle-specific acts of *Mef2-Gal4* driver, we repeated some of the key experiments using *Mhc-Gal4* (Demontis, et al., 2014) driver which is considered to be more specific to skeletal muscle and obtained similar results (Fig. S2). Other stocks used are: *Pdk1*^{3} (Rintelen, et al., 2001), *Pdk1*^{33} (Cheng, et al., 2011), *UAS-dicer2* (BL24650), *UAS-S6kRNAi* (NIG 10539R-2), *UAS-S6K*^{CA} (BL6914), *UAS-raptorRNAi* (BL31528-JF01087), *UAS-rictorRNAi* (BL31527-JF01086), *UAS-Pdk1* (Cheng, et al., 2011), *UAS-Pdk1RNAi* (BL27725-JF02807), *UAS-Tor*^{DN} (BL7013), *UAS-InR* (BL8284), *UAS-InR-RNAi* (VDRC 992).

Immunoblot analysis

Late foraging 3rd instar larvae were used for immunoblots unless otherwise noted. Four to six larval body wall tissues containing muscle-epidermis complex were homogenized in 21 µl of RIPA buffer (Sigma, #R0278) supplemented with a cocktail of protease inhibitors (Complete mini, Roche) and incubated at 4^{o}C for 40 min with agitation. After centrifugation, 13 µl of supernatant from each sample was transferred into a new tube, mixed with 7 µl of 3X loading buffer and denatured for 5 min at 95^{o}C. Equal volumes from each sample were run on 4-12% Bis-Tris gel (Novex, #NP0322BOX) and transferred onto PVDF membrane (Millipore, #IPFL00010). The

membranes were then blocked with Casein-containing buffer (Bio-Rad, #1610783) and incubated with primary antibody at 4$_{o}$C overnight. The following primary antibodies were used: rabbit anti-AKT1 (1:1000, Cell Signaling Technology, #4691), rabbit anti-pAKT1 (1:1000, Cell Signaling Technology, #4054), rabbit anti-pS6K (1:250, Cell Signaling Technology, #9209), rabbit anti-pSmad2 (1:500, Cell Signaling Technology, #3108), mouse anti-Actn (1:50, DSHB, 2G3-3D7), anti-β-Tubulin (1:1000, DSHB, E7). Secondary antibodies were HRP-conjugated anti-rabbit or mouse IgG (1:10,000, Cell Signaling Technology, #7074 and #7076, respectively). Bands were visualized using Pierce ECL Western Blotting Substrate (Thermo Scientific, #32209) and band intensities were quantified using Image J (NIH) software. The quantification graphs are presented beneath the representative immunoblot images and the data are mean ± SEM from at least three independent samplings. The title of y-axis of each graph is 'Relative protein level' and is omitted for simplification.

Immunohistochemistry

Wandering larvae were rinsed in ddH_2O and dissected in Ca^{2+}-free HL3 as described previously (Kim and O'Connor, 2014). The larval fillets were then fixed in 3.7 % Paraformaldehyde solution (Electron Microscopy Sciences) for 15 min at RT. After washing in 1X PBS and permeabilization in 1X PBT (0.5% BSA+0.2% Triton X-100 in 1XPBS), the fillets were incubated with primary antibodies overnight at 4$_{o}$C and secondary antibodies at room temperature for 2 hrs. Mouse anti-Actn antibody was used in 1:100 dilution. Alexa555-conjugated secondary antibody (Molecular Probes) was used at 1:200. Images were taken using Zeisss LSM 710 confocal microscope.

Protein synthesis assay

Surface sensing of translation (SUnSET) method (Schmidt, et al., 2009) was adopted to monitor protein synthesis capacity of the skeletal muscle with little modification. The SUnSET assay takes advantage of the fact that puromycin, a structural analog of aminoacyl-tRNA, can be incorporated into elongating polypeptide chains and can be immunologically detected. In the assay, 2-3 fillets of late foraging larvae were incubated in M3 insect medium (Sigma-Aldrich) supplemented with 2 mM of trehalose (Sigma-Aldrich), 15 μg/ml of puromycin (Sigma-Aldrich) and 10 μg/ml of insulin (Sigma-Aldrich) for 20 min at RT. The fillets were washed 3 times in 1X PBS and then sampled for immunoblotting. Anti-puromycin antibody (Millipore, #MABE343) was used at 1:10000. Representative images from triplicated assays are shown.

qRT-PCR

Seven to ten larvae were dissected in 1X PBS to remove the internal organs. Total RNAs were prepared from the remaining muscle-epidermis complexes using TRIzol reagent (Invitrogen), followed by cleanup with RNAeasy Mini kit (Qiagen). The Superscript III first-strand synthesis kit (Invitrogen) was used to synthesize cDNA and qRT-PCR reactions were performed on LightCycler 480 (Roche) using SYBR green kit. Each sample was triplicated per reaction. *Rpl23* was used as a normalization control. The fold changes were calculated based on values obtained by 2^{nd} derivative maximum method. Data are mean ± SEM from at least three independent mRNA preparations.

RNA sequencing (RNA-seq) analysis

Total RNAs were extracted using TRIzol reagent (Invitrogen) and further cleaned using RNAeasy kit (Qiagen) from thirty muscle-epidermis complexes of *wt* and *dSmad2* mutant as well as *tub-Gal80^{ts}/+;Mhc-Gal4/+* and *tub-Gal80^{ts}/+;Mhc-Gal4/babo^{CA}* animals that were heat-shocked for 12 hr at 30^{o}C for temporal expression of *babo^{CA}*. Three μgs of total RNA per genotype

were submitted to University of Minnesota Genomics Center (UMGC) for quality assessment and Illumina next-generation sequencing. In the UMGC, the integrity of RNAs was assessed using capillary electrophoresis (Agilent Bioanalyzer 2100). The sequencing libraries were constructed using TruSeq RNA preparation kit v2 after the mRNAs were enriched by oligo-dT-mediated purification. The libraries were then sequenced on a 50 bp paired-end run on the Illumina HiSeq 2500. Over 10 million reads were generated per library. The RNA-seq reads were mapped to *Drosophila* genome using TopHat. After mapping, the reads were assembled into transcripts using Cufflinks which generated fragments per kilo base of transcript per million mapped reads (FPKM) values. Gene differential expression test was performed using Cuffdiff. Finally, heat maps were drawn using R with ggplot2 package.

Statistical Analysis

Statistical analyses were performed using Prism software (version 6.0, GraphPad Software). Data are presented as Mean ± SEM. One-way ANOVA followed by Dunnett's test was used for comparisons among multiple groups and asterisks are used to denote the significance. Comparisons between two groups were performed by unpaired t-test and significances are denoted by pound signs. Graphs were drawn using either Prism or Exel software.

Results

Removal of the entire Activin signal pathway results in smaller larval muscles.

To examine how muscle size is altered in Activin pathway mutants, we counted Z-discs from the larval skeletal muscles stained with an Actn antibody. The Z-disc number is a proxy for sarcomere number and reflects the anterior-posterior length of the muscle cell. We also measured the lateral width of the muscle. The Actn antibody labels Z-discs with a similar intensity in wild-

type and Activin pathway mutant muscles (Fig. 1A), consistent with the results from immunoblot analysis (Fig. 5A). Notably, however, the surface area of each muscle cell is smaller in the *babo* and *dSmad2* mutants (Fig. 1A). Quantitatively, the *babo* and *dSmad2* muscles exhibited ~35% reduction in Z-disc number (56.16 ± 1.39 for wt vs. 36.58 ± 0.78 for *babo* and 38.58 ± 0.71 for *dSmad2*) and ~25% decrease in muscle width (1.02 ± 0.02 for wt vs. 0.79 ± 0.02 for *babo* and 0.73 ± 0.03 for *dSmad2*) (Fig. 1B), demonstrating that the Activin signaling plays an essential role in new sarcomere additions leading to muscle lengthening as well as lateral expansion of sarcomeres adding to muscle width. The muscle length and width of *babo* and *dSmad2* mutants are decreased without an accompanying change in nuclei number (Fig. S1D) indicating that the myoblast fusion occurs properly in these mutants, but the growth of individual muscle fibers is affected. Furthermore, the effect of Activin signaling on muscle length and width was found to be cell-autonomous since expression of a *dSmad2* transgene using a muscle driver restored the decreased Z-disc number and muscle width of *dSmad2* mutant (Fig. 1C). Finally, a similar reduction in the width and length of muscle cells is observed in *Actβ* mutants (Fig. 1D and (Moss-Taylor, et al., 2019)), but not in *myo* or *daw* mutants (Fig. 1D), consistent with the idea that Actβ is the major Activin-like ligand that regulates larval muscle growth in *Drosophila*. Interestingly, the skeletal muscle is disproportionately smaller when compared to other organs in *Actβ* mutants (Moss-Taylor, et al., 2019). Taken together with the finding that Activin signaling regulates muscle size in a cell autonomous manner (Fig. 1C), these results indicate that the Activin signaling regulates muscle growth independently of its influence on overall body size.

Influence of the Activin pathway on InR/dTOR signaling in larval skeletal muscle

In mammalian skeletal muscle, Mstn signaling is known to inhibit the IGF-1/PI3K/mTOR pathway (Chen, et al., 2017; Zhou, et al., 2010; Amirouche, et al., 2009). To determine if the two pathways interact similarly in non-mammalian muscle, we investigated phosphorylation of AKT1 and S6K in *Drosophila* larval skeletal muscle-epidermis complexes of wild-type and Activin pathway mutants. The pAKT1 antibody used in this study detects phosphorylation of AKT1 at Ser505. This site corresponds to Ser473 of mammalian AKT and is phosphorylated by dTORC2 (Hietakangas and Cohen, 2007; Yang, et al., 2006; Sarbassov, et al., 2005). The pS6K antibody detects phosphorylation at Thr398 which corresponds to Thr389 of mammalian S6K and is phosphorylated by dTORC1 (Lindquist, et al., 2011; Kockel, et al., 2010; Yang, et al., 2006; Sarbassov, et al., 2005). We utilized heteroallelic combination of $baob_{fd4}$ and $babo_{df}$ ($babo_{fd4/df}$), as well as $dSmad2_{F4}$/Y as TGF-β/Activin pathway mutants in which the canonical signaling is completely abolished (Fig. S1A).

We first confirmed that phosphorylation at these sites is indeed dependent on InR activity in the larval skeletal muscle by overexpressing wild-type *InR* and *InR-RNAi* using *Mef2-Gal4* driver to increase or suppress the InR activity, respectively, in the skeletal muscle. As shown in Fig. 2A, phosphorylation of AKT1 is greatly reduced by *InR-RNAi* and increased by *InR* overexpression in the muscle-epidermis complexes, confirming that the phosphorylation level at Ser505 of AKT1 faithfully reflects the InR activity. The results also indicate that dTORC2 activation is one of the downstream events of InR activation since the Ser505 of AKT1 is exclusively phosphorylated by dTORC2 (Hietakangas and Cohen, 2007; Sarbassov, et al., 2005). The phosphorylation at Thr398 of S6K is similarly regulated by InR activity, that is, decreased by *InR-RNAi* and increased by *InR* overexpression (Fig. 2A), suggesting that dTORC1 is also positively regulated by InR signaling in *Drosophila* larval skeletal muscle.

We next examined the effect of loss of *babo* and *dSmad2* on phosphorylation of AKT1 and S6K. In mammalian skeletal muscle and myoblast culture, phosphorylation of AKT at Ser473 has been shown to be negatively regulated by Myostatin-induced Activin/TGF-β signaling (Lokireddy, et al., 2011; Tan, et al., 2011; Trendelenburg, et al., 2009). We found increased phosphorylation at the corresponding site of *Drosophila* AKT1 (Ser505) in the *babo* and *dSmad2* mutants (Fig. 2B), which implies a negative effect of Activin/TGF-β signaling on AKT1 phosphorylation. The result also suggests that dTORC2 activity is elevated in *Drosophila* Activin/TGF-β pathway mutants. In contrast to AKT1, phosphorylation of S6K is mildly decreased in *babo* and *dSmad2* mutants (Fig. 2B), indicating a decreased dTORC1 activity. The influence of TGF-β/Activin signaling on phosphorylation of AKT1 and S6K appears to be muscle-specific and cell-autonomous in the muscle-epidermis complexes, since expression of a wild-type *dSmad2* transgene in the muscle of a *dSmad2* mutant resulted in a restoration of pAKT1 and pS6K levels toward those of wild-type (Fig. 2C). In addition to the continuously-feeding foraging larvae that are used for all the immunoblot analyses in this study, we also examined wandering larvae that have ceased feeding to determine if the alterations in pAKT1 and pS6K levels are dependent on feeding status. As in foraging stage, the wandering larvae of *babo* and *dSmad2* mutants also exhibited elevated pAKT1 and decreased pS6K levels (Fig. 2D). Taken together, these results indicate that the dTORC1 activity is down-regulated in Activin/TGF-β pathway mutants leading to a decreased phosphorylation of S6K (Thr398), while dTORC2 activity is upregulated resulting in an elevated phosphorylation of AKT1 (Ser505). Furthermore, the regulatory effects of Activin signaling on dTORC1 and dTORC2 activities appears to be independent of the feeding status.

Negative feedback loop by S6K

Our findings suggest that the dTORC1 and dTORC2 activities are differentially affected by the loss of canonical Activin signaling while both of them are similarly regulated by InR activity (Fig. 2A). To uncover why the phosphorylation statuses of AKT1 and S6K are changed in opposite directions, we examined if a negative feedback loop involving S6K played a role. It has been shown that mTORC1 negatively regulates the IGF-1/PI3K/AKT pathway by inducing S6K-mediated phosphorylation and degradation of insulin receptor substrate (IRS) (Harrington, et al., 2004; Um, et al., 2004). The inhibitory effect of S6K activation on AKT1 phosphorylation at Ser505 has also been demonstrated in *Drosophila* (Kockel, et al., 2010; Sarbassov, et al., 2005). Since the S6K activity is likely decreased in Activin pathway mutants judged by reduced phosphorylation at T398 (Fig. 2B) and the fact that there is lower protein synthesis capacity in these mutants (see below), it is possible that the elevated pAKT1 level in *babo* and *dSmad2* muscles is an indirect result of weakened inhibitory feedback of S6K on the InR-AKT1 axis. To test this possibility, we overexpressed an activated form of S6K ($S6K_{CA}$) in *dSmad2* muscle to compensate for the decreased S6K activity and found that it decreases pAKT1 levels towards that of wild type (Fig. 3A). In addition, knockdown of *S6k* in wild-type muscle increased pAKT1 level while overexpression of $S6k_{CA}$ decreased it (Fig. 3B). To further demonstrate the importance of negative feedback on the phosphorylation status of AKT1 at Ser505, we suppressed the dTORC1 activity by knocking-down *raptor*, a key component of dTORC1, and observed an increase in the pAKT1 level (Fig. 3C). Knocking-down *rictor*, a crucial component of dTORC2 complex, on the other hand, led to a decreased phosphorylation of pAKT1, further confirming that dTORC2 is the primary player in phosphorylating AKT1 at this site (Fig. 3C). Taken together, these results demonstrate that the elevated AKT1 phosphorylation in *babo* and *dSmad2* muscles is a consequence of decreased activity of dTORC1 and S6K. Finally, we investigated the protein

synthesis capacity of wild-type and TGF-β/Activin pathway mutants which is known to be controlled by TORC1 and S6K activities. By adopting the SUnSET method (Schmidt, et al., 2009), we find that protein synthesis capacity is reduced in the body wall tissue of *babo* and *dSmad2* mutants (Fig. 3D). Furthermore, the decreased capacity in protein synthesis was rescued by muscle specific expression of wild type *dSmad2* in a *dSmad2* mutant (Fig. 3E). These results further demonstrate that the activities of dTORC1 and S6K, both key regulators of protein synthesis, are downregulated in the muscle of TGF-β/Activin pathway mutants.

Transcriptional regulation of InR/dTOR pathway components by Activin signaling

Considering that dSmad2, the R-Smad of the Activin/TGF-β pathway, is a transcription factor, one possibility is that the *Drosophila* Activin/TGF-β pathway influences the InR/dTOR pathway via transcriptional control of one or more of its signal transduction component(s). To gain insight into the transcriptional influence of the Activin/TGF-β pathway on InR/dTOR signaling, we performed RNA-seq using wild-type and *dSmad2* mutant as well as *Mhc-Gal4;tub-Gal80ts* control and *babo*^{CA} gain of function-expressing samples. The heat map using FPKM values of genes encoding InR/dTOR signaling components shows that transcripts of *Pdk1* and *Akt1* are significantly decreased while transcription of the rest of the genes are unaffected in a *dSmad2* mutant suggesting a positive role of Activin/TGF-β pathway on the transcription of specific sets of genes in the InR/dTOR signaling pathway (Fig. 4A). In addition, temporal expression of activated Babo led to an increase in the transcripts of *Pdk1* and *Akt1* further demonstrating the positive role of Activin/TGF-β pathway (Fig. 4A). The RNA-seq results were then validated by qPCR analysis which also exhibited a decrease in the transcripts of *Pdk1* and *Akt1* (Fig. 4B). Consistent with the findings from RNA-seq and qPCR analyses, the total protein level of AKT1 was found to be decreased in *babo* and *dSmad2* mutants (Fig. 4C), even though the pAKT1 level

is elevated in these mutants (Fig. 2B). Taken together, these results suggest that the Activin pathway impinges on InR/dTOR pathway via controlling the transcription of some of its signal transduction components.

In order to determine if the decrease in the transcripts of InR/dTOR signaling components is responsible for any of the phenotypes exhibited by Activin pathway mutants, we sought to restore the expression level of *Pdk1* in the *dSmad2* muscle and examined pAKT1 (Ser505) level that inversely correlates with dTOCR1 and S6K activities (Fig. 3). As shown in Fig. 4D, overexpressing *Pdk1* in *dSmad2* muscle reduced the elevated pAKT1 level toward that of wild type, suggesting that the decrease in the expression of *Pdk1* is, at least partly, responsible for the elevated phosphorylation of AKT1. In a converse experiment, *Pdk1* was either knocked-down or overexpressed in otherwise wild-type muscles and the phosphorylation of AKT1 was examined. In line with the idea that *Pdk1* expression level negatively correlates with AKT1 phosphorylation, *Pdk1* knockdown increased the pAKT1 level while *Pdk1* overexpression decreased it (Fig. 4E). Since we showed above that the pAKT1 level also negatively correlates with S6K activity (Fig. 3B). Since the S6K activity is enhanced upon phosphorylation at active site (Thr238) by PDK1 as inferred from mammalian results (Pullen, et al., 1998), we propose that the effect of changes in *Pdk1* expression on pAKT1 phosphorylation is likely ascribed to the alterations in S6K activity. Finally, AKT1 phosphorylation is also found to be increased in *Pdk1* mutant (Fig. 3F) further supporting the idea of negative correlation between PDK1 activity and pAKT1 level. All together, these results suggest that an alteration in the expression of downstream signal transduction components can significantly affect the output of InR/dTOR signaling pathway even in the absence of a change in the ligand availability or activity and this appears to be the mechanism by which the Activin pathway influences the InR/dTOR signaling.

Effect of Activin/TGF-β pathway on sarcomeric protein levels

In mammals, the Mstn /Activin pathway has been shown to negatively regulate MHC levels which in turn correlate with the change in muscle size in mammalian myoblast culture and skeletal muscle (Hulmi, et al., 2013; Lokireddy, et al., 2011). We examined if the Activin pathway similarly affects MHC levels in *Drosophila* muscle. In the immunoblot analysis using muscle-epidermis tissue, *babo* and *dSmad2* mutants exhibited reduced MHC abundance (Fig. 5A), even though the transcript level of *Mhc* is not changed (Fig. S1B). Furthermore, expressing a wild-type *dSmad2* transgene in *dSmad2* muscle rescued the decreased MHC level, indicating a tissue-autonomous effect of the Activin pathway (Fig. 5C). In contrast, the total amount of Actinin (Actn), another sarcomeric protein, is not altered in *babo* and *dSmad2* mutants (Fig. 5A) despite the increase in its transcript level (Fig. S1B). Therefore, it appears that the Activin pathway has variable effects on protein and transcript levels of different sarcomeric proteins. Specifically, the Activin pathway either positively regulates the translation or suppresses the degradation of MHC in *Drosophila* larval skeletal muscle.

As shown above, a decrease in *Pdk1* expression gives rise to altered InR/dTOR signaling in *babo* and *dSmad2* mutants. Since the InR/dTOR signaling has a role in protein synthesis and degradation, we investigated if the decrease in *Pdk1* expression also contributes to the change in MHC level found in Activin pathway mutants. As illustrated in Fig. 5B, knockdown or overexpression of *Pdk1* resulted in decreased and increased levels of MHC, respectively, demonstrating a positive relationship between *Pdk1* expression and MHC protein levels. We then overexpressed *Pdk1* in *dSmad2* muscle and found that it rescues the decreased MHC level (Fig. 5C). From these results, we conclude that the decrease in *Pdk1* expression is, at least in part, responsible for the reduced MHC level shown by Activin pathway mutants.

We found that decreased *Pdk1* expression leads to diminished dTORC1 activity in Activin pathway mutants as illustrated by inversely correlating pAKT1 level (Fig. 4D and E). To investigate the contribution of dTORC1 in the regulation of MHC level by the Activin pathway, we expressed dominant negative *Tor* (*Tor^{DN}*) together with activated *babo* (*babo^{CA}*). Activated Babo alone increased the MHC production by 2-fold, which was suppressed by co-expression of *dSmad2RNAi* (Fig. 5D), meaning that the Babo^{CA} promoted MHC production primarily through canonical dSmad2-dependent signaling. Interestingly, co-expression of *Tor^{DN}* resulted in an even stronger suppression of the hyper-MHC production induced by Babo^{CA} (Fig. 5D). Furthermore, a similar result was obtained by co-expression of *babo^{CA}* and *raptorRNAi* (Fig. S1E) suggesting that dTORC1 activity mediates almost all of the effect of Babo^{CA} on the MHC level. Finally, we overexpressed *S6k^{CA}* in *dSmad2* mutant muscle to increase the activity of S6K and found that it rescues the MHC level (Fig. 5C). These result further emphasizes the importance of dTORC1-S6K axis in mediating the effect of Activin pathway on MHC abundance.

Activin signaling promotes muscle growth through both InR/dTORC1 dependent and independent mechanisms

The findings that dTORC1 signaling, as well as MHC levels, are downregulated in Activin pathway mutants, led us to hypothesize that the reduction in MHC via the reduced dTORC1 signaling is primarily responsible for the decrease muscle growth observed in Activin pathway mutants. As shown above, the decreased MHC level of *dSmad2* muscle is rescued by overexpression of *Pdk1* and *S6k^{CA}* (Fig. 5C). Because MHC is an essential building block of sarcomeres, we reasoned that overexpression of *Pdk1* or *S6k^{CA}* would rescue the sarcomere number of *dSmad2* muscle. Surprisingly, however, overexpression of either of these transgenes failed to

rescue the sarcomere number as assayed by counting the Z-discs in *dSmad2* muscle (Fig. 6A). Furthermore, the *S6k*^{CA} even further decreased the sarcomere number from that of control *dSmad2* mutant muscle (Fig. 6A). Therefore, these results indicate that sarcomere formation can be decoupled from sarcomeric protein production and also suggests that the Activin pathway promotes sarcomere formation independently of its influence on InR/dTORC1 signaling and MHC production. Interestingly, overexpression of *Pdk1* or *S6k*^{CA} increased the width of *dSmad2* muscle (Fig. 6A). From these results, we suggest that if MHC is over-produced in the absence of canonical Activin signaling, it is used for lateral expansion of the muscle likely through addition to existing sarcomeres.

To further test the decoupling between the abundance of sarcomeric protein components and sarcomere number, we overexpressed *S6kRNAi* or *S6k*^{CA} in otherwise wild-type muscle to alter the S6K activity. In line with the essential role of S6K in regulating MHC production, expression of *S6kRNAi* and S6K^{CA} caused a significant decrease and increase in MHC levels, respectively (Fig. 6B). As in *babo* and *dSmad2* mutants, the Actn level is not affected by alterations in the S6K activity (Fig. 6B). Despite profoundly affecting the MHC abundance, neither *S6kRNA*i nor *S6k*^{CA}, had much effect on the Z-disc number (Fig. 6C), further demonstrating the lack of correlation between MHC production and serial sarcomere formation. Finally, we counted Z-discs in the muscles expressing *babo*^{CA} together with *dSmad2RNAi* or *Tor*^{DN}. Overexpressing *babo*^{CA} alone causes an increase in the MHC level by 2-fold which was suppressed by co-expressed *dSmad2RNAi* or *Tor*^{DN} (Fig. 5D). In the Z-disc counting assay, *babo*^{CA}-expressing muscles exhibited, on average, 20 more sarcomeres than the *Mef-Gal4* controls (70.9 ± 1.43 for *Mef2>+* vs. 89.45 ± 0.91 for *Mef2>babo*^{CA}; Fig. 6D). As expected, *dSmad2RNAi* completely blocked the increase in sarcomere number caused by *babo*^{CA} overexpression and even further reduced the

sarcomere number from that of control (89.45 ± 0.91 for *Mef2>babo^{CA}* vs. 61 ± 0.72 for *Mef2>babo^{CA}+dSmad2RNAi* vs. 70.9 ± 1.43 for *Mef2>+*; Fig. 6D). In contrast, the *Tor^{DN}* only mildly suppressed the effect of *babo^{CA}* so that the sarcomere number is still higher than that of control (89.45 ± 0.91 of *Mef2>babo^{CA}* vs. 79.63 ± 2.13 for *Mef2>babo^{CA}+Tor^{DN}* vs. 70.9 ± 1.43 for *Mef2>+*; Fig. 6D). Considering that the *Mef2>babo^{CA}+Tor^{DN}* muscle likely has a higher level of Activin signaling but has a lesser amount of MHC (Fig. 5D) than the *Mef2>babo^{CA}+dSmad2RNAi* and *Mef2>+* control muscles, we conclude that the sarcomere number better correlates with the level of Activin signaling than with sarcomeric protein abundance. In contrast to the sarcomere number, muscle width is reduced by *babo^{CA}* overexpression and *dSmad2RNAi* rescued it (Fig. 6D). We rationalize that the muscle width is smaller in *babo^{CA}*-overexpressing muscle to accommodate the large increase in sarcomere number. In other words, sarcomeric subunits are assembled into new sarcomeres expanding the muscle length at the expense of widening of muscle through addition of sarcomeric proteins into existing Z-discs.

Discussion

In this study, we assessed the effect of canonical *Drosophila* Activin signaling on InR/dTOR pathway activity and its relation to larval body-wall muscle growth. Our findings reveal an unexpected and striking difference in way that Activin signaling regulates muscle size in *Drosophila* larvae compared to mammals. In *Drosophila*, Activin signaling promotes muscle growth while in developing mammals it limits muscle mass. As in mammals, we find that the InR/TORC1 pathway is a core conserved target that mediates muscle size control in response to Activin, but the activity of the IGF-1/TORC1 pathway is regulated in opposing directions in the

two systems. In *Drosophila*, Activin signaling enhances the expression of *Pdk1* and *Akt1* two essential components of the InR/dTORC1 pathway and thereby stimulates pathway activity, while in mammals the activity of IGF-1/mTORC1 pathway is down regulated by Myostatin/Activin signaling (Chen, et al., 2017; Zhou, et al., 2010; Amirouche, et al., 2009). We also find that stimulation of InR/dTORC1 signaling in *Drosophila* in the absence of Activin leads to up-regulation of MHC which is incorporated into existing sarcomeres to increase their width. However, in the presence of Activin signaling both the width and length of muscle fibers are enhanced. The combinatorial effect of these two sarcomeric assembly processes is the formation of larger larval body wall muscles with an increased surface area.

Differential modulation of IGF-1/TORC1 pathway accounts for the opposing effects of Activin signaling on mammalian verses *Drosophila* somatic muscles size.

The present study demonstrates that the Activin pathway in *Drosophila* controls the output of the InR pathway by regulating the expression level of PDK1 and AKT1, two downstream InR signal transduction components (Fig. 4). Since the steady-state levels of these two transcripts are lower in the body walls of *dSmad2* and *babo* mutants, and are increased by expression of an activated Babo in muscle, it seems likely that these two genes are direct transcriptionally-regulated targets of dSmad2, although we cannot rule out more complicated scenarios involving regulation of message stability. In either case, the net result is that Activin signaling boosts InR/dTORC1 activity resulting in enhanced S6K activity, higher general levels of protein synthesis and increased levels of MHC. When reception of Activin signaling is compromised, then the opposite occurs. (Fig. 2 and 3). This mechanism is quite different from what has been proposed for how Mstn/Activin signaling impinges on the insulin/IGF-1 activity

in mammals. In general, it has been reported that AKT phosphorylation is upregulated in the absence of Mstn/Activin signaling (Hitachi, et al., 2014; Tan, et al., 2011). Other points of intersection between the pathways have also been reported including several studies in mice suggesting that Mstn/Activin signaling suppresses expression of miRNAs that inhibit the *PTEN* translation (Hitachi, et al., 2014; Goodman, et al., 2013). This leads to lower levels of AKT phosphorylation, decreased mTORC1 activation and smaller muscles in the presence of Mstn/Activin signals.

Why mammals and *Drosophila* are wired in opposite directions in terms of Activin's signaling influence on IGF-1/TORC1 activity and muscle size control is unclear. The Mstn/ Activin branch of the TGF-β family is very ancient and is present in some pre-Bilateria groups including several cnidarian species (Watanabe, et al., 2014), but functional studies of its role in muscle size control in these animals are lacking. In fact, Mstn's role in muscle growth has only been studied in a few other non-mammalian vertebrates including chickens, turkeys and zebrafish where the results mirror the mammalian case (Bhattacharya, et al., 2019; Gao, et al., 2016; McFarland, et al., 2006). As for invertebrates, there are two published reports, one using the giant prawn *Macrobrachium rosenbergii* (Easwvaran, et al., 2019) and the other the penaeid shrimp *Penaeus monodon* (De Santis, et al., 2011). Despite both species being members of the Malacostraca class of Crustacea, these studies reached opposite conclusions. Mstn had an apparent positive role in body growth in *Penaeus* (De Santis, et al., 2011), similar to what we see in *Drosophila*, while in *Macrobrachium* it had a negative effect on muscle size similar to what is observed in mammals (Easwvaran, et al., 2019). Clearly, many additional phyla, classes and species of animals need to be examined to more fully understand how and why these contrasting roles in muscle size control have evolved.

The IGF-1/TORC1 pathway is only one point of intersection from which to understand muscle size control. In general, muscle homeostasis is thought to be regulated by balancing the activities of protein synthesis and degradation pathways (Bonaldo and Sandri, 2013; Schiaffino and Mammucari, 2011). The IGF-1/TORC1 signaling clearly interfaces with both these modes of protein homeostasis control, however, in most cases it is not clear whether Smad directly regulates expression of specific components in either the synthesis or degradation pathways or whether most of its affects can be attributed to regulation of IGF-1/TORC1. In addition, it is not clear to what extent non-canonical modes of TGFβ signaling, of which there are many in the vertebrates [reviewed in (Zhang, 2009)] but few in *Drosophila* (Ng, 2008; Eaton and Davis, 2005), might come into play in regulating protein homeostatic balance.

IGF-1/TORC1 negative feedback and muscle homeostasis?

It is well documented in mammals that there is a negative feedback loop formed by S6K toward IRS which profoundly diminishes the efficacy of signaling from insulin/IGF-1 to PI3K-AKT axis (Zhang, et al., 2008; Harrington, et al., 2004; Shah, et al., 2004). A similar negative feedback loop has also been demonstrated in *Drosophila* cell culture (Sarbassov, et al., 2005) and wing imaginal discs (Kockel, et al., 2010), but has never been studied in skeletal muscle. Here we demonstrate that this negative feedback loop does indeed work efficiently in *Drosophila* skeletal muscle. As the inhibitory feedback has a profound effect on insulin responsiveness, it will be interesting to determine how the peripheral tissues in Activin pathway mutants react to *Drosophila* insulin-like peptides. Together with the fact that the absolute expression level of PDK1 and AKT1 are down-regulated in the Activin pathway mutants, it may not be a resultant enhancement of the responsiveness. Consistent with the idea, we previously reported that the *dSmad2* as well as *daw* mutants display increased hemolymph sugar levels (Ghosh and O'Connor, 2014), suggesting an

impairment in the regulation of blood sugar level. In addition, it might also indicate that the decrease in PDK1 and AKT1 expression overrides the effect of relieved negative feedback. Further study is required to unveil how these competing effects are summed by tissues to determine their responsiveness to insulin or other growth factors.

Which Ligands control muscle size in *Drosophila* verses mammals

In mammals, the TGFβ superfamily consists of at least 30 ligands which are broadly classified into two signaling groups base on phylogenetic analysis and biochemical assays. These are the BMPs that transduce signals through Smads1,5,8 and members of the TGFβ/Activin subgroup, including Mstn, that signal through Smads2 and 3 (Sartori, et al., 2014). The *Drosophila* system is much simpler with only 6 clear family members, three of which are classified as BMPs and three that belong to the Activin subgroup including Myoglianin, the homolog of vertebrate Mstn (Upadhyay, et al., 2017). In vertebrates, the full complement of ligands that participate in muscle size control in not known. For the purpose of this discussion we use the term "size control and "muscle growth" to refer only to fiber size regulation post differentiation, not changes in fiber number which occur during myogenesis or when muscle satellite cells are activated in response to muscle injuries, which are also influenced by TGF-β signaling. Mstn is by far the best-studied family member in terms of post-myogenic muscle growth control, however several lines of evidence suggest that other Activins, as well as BMP family members, also participate in muscle size homeostasis. These studies employed follistatin and a dominant negative ActRIIB, both of which bind to several Activins and BMPs blocking their ability to form functional signaling complexes. Overexpression of these inhibitors in mice produced more extreme muscle hypertrophy than the *mstn* knockout alone (Winbanks, et al., 2012; Lee, et al., 2005; Lee and McPherron, 2001), implicating that other TGFβ factors

likely contribute to muscle growth control. More recently, administration of a specific Activin A inhibitor to mice was also shown to produce muscle hypertrophy clearly implicating this family member as regulator of muscle growth. (Chen, et al., 2017; Chen, et al., 2015; Chen, et al., 2014).

While the BMP arm of the superfamily has not received as much attention, overexpression of BMP-7 or its activated type I receptor in muscles resulted in enhanced Smad1,5,8 phosphorylation and hypertrophic muscle growth (Stantzou, et al., 2017; Sartori, et al., 2013; Winbanks, et al., 2013). Intriguingly, this appears to be accomplished, in part, through mTORC1 activation, increased protein synthesis, and reduced protein turnover, very similar to what we find for the Activin pathway in *Drosophila*. At present, no specific studies addressing the role of BMPs in muscle growth control have been reported in *Drosophila*, although it is worth noting that the BMP-7 homolog, Gbb, is expressed in larval muscle and strongly affects NMJ size and function (McCabe, et al., 2003). However, in these studies no specific alterations in muscle proportions and/or sarcomeric number were reported. In fatbody, however, Gbb has been shown to inhibit insulin signaling by inducing the expression of *tribbles*, a negative regulator of AKT1 (Hong, et al., 2016). Whether this also occurs in muscle remains to be examined.

In terms of three *Drosophila* Activin-like ligands, muscle size regulation appears to be primarily accomplished by motoneuron delivery of Actβ to the muscle during larval growth (Moss-Taylor, et al., 2019). Loss of Actβ results in reduction of larval muscle size to a similar extent as we report here for Babo and dSmad2 loss, while genetic null mutations in either *myo* or *daw*, the other two activin-like ligands, produces no change in muscle size (Fig. 1D). Furthermore, loss of Actβ also results in similar electrophysiological defects at the NMJ as found

for *babo* and d*Smad2*, while loss of Daw or Myo have little effect (Kim and O'Connor, 2014). These data all support Actβ as the primary *Drosophila* TGFβ-like ligand involved in muscle size control.

It is surprising that we find no effect of *myo* loss on muscle size since it is a clear homolog of vertebrate Mstn. Furthermore, it has been reported that RNAi knockdown of *myo* in muscles does result in a size increase, (Augustin, et al., 2017). These results are consistent with a negative role for Myo similar to Mstn its vertebrate counterpart. At present, we do not know why the RNAi results are different from the genetic null data. One might expect if Myo acts as a negative muscle growth regulator and Actβ as a positive factor then loss of either *babo* or *dSmad2*, which transduce the signal for of these ligands, would result in a relatively normal size muscle, which is not what we observe. Furthermore, in *Actβ, myo* double mutants, we see little or no suppression of the *Actβ* small muscle phenotype as would be expected if Myo was a negative regulator of muscle mass (M-J Kim unpublished). Discrepancies between the tissue-specific RNAi knockdown and genetic null phenotypes have been reported quite frequently in both *Drosophila* and vertebrates. One possible explanation is the activation of compensatory pathways in the null mutant that are not elicited by tissue specific knockdown methods (El-Brolosy, et al., 2019; El-Brolosy and Stainier, 2017; Di Cara and King-Jones, 2016; Gibbens, et al., 2011).

Mechanisms of skeletal muscle growth: *Drosophila* vs mammals

The shape of *Drosophila* larval and mammalian skeletal muscle cells are very different from each other. The *Drosophila* larval body wall muscle cells have a thin single layer paper-like shape (Fig. 1A), and thus their sizes are estimated by the surface area. As we show here, differentiated muscle cells can grow by expanding either their length and/or width. In contrast,

differentiated mammalian skeletal muscle cells (myofibers) are rod-shaped and contain many myofibrils which are also rod-shaped (Haun, et al., 2019). Most mammalian skeletal muscles are singly innervated, and their myofibers extend continuously from one tendon to the other. In the adult stage, these singly innervated skeletal muscles grow by increasing the diameter not the length of each myofiber (Timson and Dudenhoeffer, 1990; Gollnick, et al., 1981). Mammals also have multiply innervated skeletal muscles such as the mouse gracilis anterior muscle (Paul and Rosenthal, 2002). The myofibers in the multiply innervated muscles terminate intrafascicularly and do not extend the entire length between tendons. These multiply innervated muscles grow by elongating the lengths and not the width of myofibers resulting in the increased number of fibers in cross section (Paul and Rosenthal, 2002).

The structural difference between *Drosophila* and mammalian skeletal muscle cells raises the issue of to what extent the mechanisms discovered to underlie muscle growth in one system can inform those of the other. In our study, the finding that TGF-β/Activin mutants bear fewer numbers of sarcomeres (Fig. 1B) implicates that TGF-β/Activin pathway promotes addition of new sarcomeres tandemly to existing ones which leads to lengthwise growth of the muscle cells. In addition, the lateral width of each sarcomere is shorter in *babo* and dSmad*2* mutants (Fig. 1A and B) meaning that TGF-β/Activin signaling also promotes the lateral expansion of sarcomeres, probably by inducing the addition of sarcomeric subunits to existing sarcomeres in a side-by-side fashion. Taken together, these results argue that the growth of larval muscle cells in both width and length occurs through the sarcomeric unit.

Unlike *Drosophila* body wall muscle cells whose growth is achieved by expanding the surface area, myofibers in singly-innervated skeletal muscles of the mammals grow by increasing the diameter, and thus the size of such myofibers has been assessed by measuring either the

diameter [(Winbanks, et al., 2012) for example] or the cross-sectional area (CSA) [(Tando, et al., 2016) for example]. Although these methods of assessment are easy to perform, they do not reveal the detailed mechanism on how changes in myofiber size are accomplished. Since the myofibers contain a number of myofibrils (Haun, et al., 2019), hypertrophy could occur either by increasing the number of myofibrils or by increasing the diameter of myofibrils in each myofiber, and simply measuring the myofiber diameter or CSA cannot differentiate between these two mechanisms. There are very few reports that have examined the number and diameter of myofibrils in myofibers, but one study showed a simultaneous increase in the number and diameter of myofibrils in hypertrophic myofibers induced by bupivacaine injection (Rosenblatt and Woods, 1992). If the myofibers grow by increasing the myofibril number, then new myofibrils are expected to be seeded somewhere in the sarcoplasm and to elongate to the full length of the myofiber, resulting in higher number of the myofibrils. Based on the structure of the myofibrils (Haun, et al., 2019), we can imagine that sarcomeres need to be added tandemly to the seeded sarcomeric structure for the elongation of myofibrils. The process hence resembles what happens during lengthwise growth of the *Drosophila* body wall muscle cells. On the other hand, if the myofibril diameter is what grows, the sarcomeric structures are expected to be added laterally to existing myofibrils, which simulates the widthwise growth of *Drosophila* muscle cells. As for multiply-innervated muscles, elongation of myofibers is the major mechanism of growth (Paul and Rosenthal, 2002), and thus the sarcomeres should be added tandemly to existing ones which again simulates the lengthwise growth of *Drosophila* muscle cells. Taken together, these observations lead us to suggest that both *Drosophila* and mammalian skeletal muscle cells, despite their differences in the shape, may utilize a common set of subcellular processes for myofiber growth, that is, adding sarcomeric structures either tandemly or in a side-by-side fashion to the existing sarcomeres. Accordingly, observations

using *Drosophila* muscle growth as a model may contribute to understanding the regulatory mechanisms of mammalian muscle growth and vice versa.

In particular, the role of Mstn/Activin signaling on myofiber size control will be interesting to examine in mammals. As demonstrated in this report, we find that both the length and width growth of *Drosophila* muscle cells are regulated by the Activin pathway. Widthwise growth is promoted by Activin's up-regulation of InR/dTORC1 signaling which in turn increases MHC production, and likely other sarcomeric molecules, and these tend to be used in lateral expansion of the sarcomeres when the Activin signal remains at a certain level. Previous observations in which AKT1 activity was manipulated through expression of its inhibitor Tribbles also supports the idea that InR/dTORC1 pathway promotes widthwise growth (Das, et al., 2014). If however, activated Babo is expressed in muscle, then there is a significant increase in the sarcomere number even when it is co-expressed with Tor^{DN} (Fig. 6D) which suppresses MHC production well below that of control (Fig. 5D). Therefore, we conclude that the lengthwise growth is also promoted by Activin signaling but it is at least partially independent of the InR/dTORC1 pathway and is also able to promote serial addition of sarcomeres even when the sarcomeric materials are reduced (Tor^{DN} + Babo^{CA} expression).

How the serial vs lateral addition of sarcomeres is differentially regulated is not clear since no studies concerning this issue have been published. Interestingly, it has recently been reported that overexpression of the PR isoform of Zasp52, a *Drosophila* ALP/Enigma family protein, results in an increased myofibril diameter in adult indirect flight muscle (González-Morales, et al., 2019), indicating that Zasp52-PR promotes the lateral expansion of sarcomeres. The result, however, does not give an insight into whether Zasp52-PR is also involved in serial addition of sarcomeres that will cause lengthening of the muscle, since the observation is limited to adult indirect flight muscle

whose length is pre-determined during the pupal stage. In addition to Zasp52 isoforms, the effects of other Zasps were also investigated in this study and it was found that overexpression of Zasp66 or Zasp67 increases the population of myofibrils having either smaller or larger diameters, indicating that these two Zasps have dual roles in determining myofibril diameter. Interestingly, we found that Zasp66 expression is decreased in larval skeletal muscle of *babo* and *dSmad2* mutants (Fig. S1F) which may be contributing to the muscle size phenotypes. Further study is required to reveal the exact role(s) of Zasp66 in the regulation of muscle growth.

In summary, we envision a two-step mechanism for how Activin controls *Drosophila* muscle fiber growth (Fig. 7). On the one hand, it regulates production of muscle fiber structural subunits such as MHC through enhancement of *Akt1* and *Pdk1* transcript levels. These subunits can be assembled laterally to build muscle fiber width. In a second step, we propose that it either positively regulates the production of a serial assembly component or blocks the destruction of such a component leading to length wise addition of new sarcomeric units. It is important to recognize that although some physiological defects have been noted in muscles of *Actβ, dSmad2* and *babo* mutants (Kim and O'Connor, 2014), these do not cause visibly noticeable changes in either larval motion or feeding behaviors. Therefore, just as in the case of mammalian Mstn signaling, *Drosophila* Activin signaling is not essential for earlier steps of myoblast fusion and muscle differentiation and function, rather it appears to be a mechanism for fine-tuning muscle fiber growth. Understanding what types of internal and external cues regulate this pathway during *Drosophila* development and perhaps adult stages may reveal new ideas on how to manipulate this pathway in humans to achieve effective therapeutic intervention for various types of muscle wasting syndromes associated with ageing and disease.

Figure legends

Fig. 1. Activin signaling is necessary for proper muscle growth. (A) Representative images of muscle 6 of abdominal segment 2 of *wt* and Activin/TGF-β pathway mutants stained with Actn antibody. Scale bar equals 50 μm. (B) Assessment of muscle length by counting Z-discs and measurement of relative width of the muscle 6 of abdominal segment 2. Both the Z-disc number and muscle width are decreased in *babo* and *dSmad2* mutants. (C) Restoring Activin signaling in *dSmad2* muscle by expressing a wild-type *dSmad2* transgene rescues the reduced Z-disc number and muscle width. (D) Only *Actβ* mutant among others displays reduction in Z-disc number and muscle width. Values are mean ± SEM. *p<0.05 and ***p<0.001 from one-way ANOVA followed by Dunnett's test in which each genotype was compared to *wt*. Additionally, unpaired t-tests were performed in C as indicated by lines. ##p<0.01 and ###p<0.001 from unpaired t-test.

Fig. 2. Activin pathway regulates the InR/dTOR signaling in the body wall. Representative immunoblot images and quantification of pAKT1 and pS6K. (A) Phosphorylation of AKT1 at S505 and S6K at T398 sites are down- and up-regulated by muscular expression of *InR-RNAi* and *InR*, respectively, suggesting that the InR signaling positively regulates the phosphorylation at these sites. (B) Phosphorylation of AKT1 is increased whereas the pS6K level is decreased in the larval body walls of *babo* and *dSmad2* mutants. (C) Resupply of Activin signaling in *dSmad2* muscle restores pAKT1 and pS6K levels close to wild type. (D) Wandering larvae display the same pattern of alteration in the AKT1 and S6K phosphorylation in the larval body wall as foraging larvae. Values are mean ± SEM. *p<0.05, **p<0.01 and ***p<0.001 from one-way ANOVA followed by Dunnett's test in which each genotype was compared to *Mef2-Gal4/+* control (A) or

wt (B, C and D). Additionally, unpaired t-tests were performed in C as indicated by lines. ##p<0.01 and ###p<0.001 from unpaired t-test.

Fig. 3. Increased phosphorylation of AKT1 is an indirect result of reduced inhibitory feedback by S6K. (A) Overexpressing a constitutively active form of *S6k* (*S6k*$_{CA}$) suppresses the hyper phosphorylation of AKT1 in *dSmad2* mutant muscle. (B) Overexpression of *S6kRNAi* and *S6k*$_{CA}$ in wild-type muscle causes hyper-phosphorylation and hypo-phosphorylation of AKT1, respectively, indicating that the negative feedback loop from S6K to InR-AKT1 axis is functioning efficiently in larval body wall muscle. (C) Overexpression of *raptorRNAi* to inhibit dTORC1 activity results in an elevated pAKT1 level while *rictorRNAi* inhibits dTORC2 activity leading to decreased phosphorylation of AKT1. (D) The larval body wall tissue of Activin pathway mutants exhibits lower protein synthesis capacity assayed by SUnSET method. (E) Rescue of decreased protein synthesis capacity by muscle specific expression of *dSmad2* transgene. Values are mean ± SEM. *p<0.05 from one-way ANOVA followed by Dunnett's test in which each genotype was compared to *wt* (A) or *UAS-dicer2/+; Mef2-Gal4/+* control (B and C). Additionally, an unpaired t-test was performed in A as indicated by lines. ##p<0.01 from unpaired t-test.

Fig. 4. Activin signaling promotes the transcription of the InR/dTOR pathway components *Pdk1* and *Akt1*. (A) The heat map shows the effects of *dSmad2* loss and temporal over-expression of *babo*$_{CA}$ on the transcript levels of InR/dTOR pathway components. While most of the components are not affected, the expression of *Pdk1* and *Akt1*, highlighted by a red rectangle in the heat map, are downregulated by *dSmad2* mutation and upregulated by temporal expression of *babo*$_{CA}$. (B) Verification of the RNA-seq results by qPCR. (C) Consistent with the RNA-seq and

qPCR results, the total protein level of AKT1 is decreased in *babo* and *dSmad2* mutants. (D) Overexpression of *Pdk1* in *dSmad2* muscle restores the increased pAKT1 level towards that of wild type. (E) Expression of *Pdk1RNAi* in the skeletal muscle produces a similar phenotype in pAKT1 level as loss of Activin signaling while *Pdk1* overexpression suppresses the AKT1 phosphorylation. (F) A heteroallelic combination of *Pdk1* mutations causes hyper phosphorylation of AKT1. Values are mean ± SEM. *p<0.05, **p<0.01 and ***p<0.001 from one-way ANOVA followed by Dunnett's test in which each genotype was compared to *wt* (B, C, D and F) or Mef*2-Gal4/+* control (E). Additionally, unpaired t-tests were performed in D and F as indicated by lines. ###p<0.001 from unpaired t-test.

Fig. 5. Activin signaling positively regulates MHC production through its effect on InR/dTOR1 activity. Representative immunoblot images and quantification of sarcomeric proteins. (A) The amount of MHC, a key sarcomeric protein, is decreased in the larval body walls of *babo* and *dSmad2* mutants while Actn, another sarcomeric protein that localizes to Z-discs, is not affected by these mutations. (B) Muscle expression of *Pdk1RNAi* decreases MHC abundance while expressing wild-type *Pdk1* in the muscle increases it, indicating a positive correlation between *Pdk1* expression level and the amount of MHC. (C) Expressing *dSmad2*, *Pdk1* and $S6k_{CA}$ transgenes in *dSmad2* mutant muscle rescues the decreased MHC level. (D) Expressing $babo_{CA}$ causes hyper-production of MHC which is suppressed by co-expression of *dSmad2RNAi* or Tor_{DN}. Values are mean ± SEM. *p<0.05, **p<0.01 and ***p<0.001 from one-way ANOVA followed by Dunnett's test in which each genotype was compared to *wt* (A), *Mef2-Gal4/+* control (B and D) or *Mef2-Gal4/+* control in *dSmad2* mutant background (C). Additionally, unpaired t-tests were performed in D as indicated by lines. ##p<0.01 and ###p<0.001 from unpaired t-test.

Fig. 6. Z-disc number is decoupled from MHC level

(A) Overexpression of *Pdk1* and *S6k^{CA}* in *dSmad2* muscles rescues the muscle width but not the Z-disc number. (B) Expression of *S6kRNAi* and *S6k^{CA}* in wild-type muscle reduces and increases the MHC level, respectively, with no effect on the Actn level. (C) Although the *S6kRNAi* and *S6k^{CA}* profoundly affect the MHC level in larval body wall tissue, they have no or little effect on Z-disc number of the muscle. However, the muscle width is significantly reduced by *S6kRNAi* and increased by *S6k^{CA}* expression . (D) Z-disc number and relative width of the muscles expressing *babo^{CA}* alone and together with *dSmad2RNAi* or *Tor^{DN}*. Values are mean ± SEM. *p<0.05, **p<0.01 and ***p<0.001 from one-way ANOVA followed by Dunnett's test in which each genotype was compared to *Mef2-Gal4/+* control (D) or *Mef2-Gal4/+* control in *dSmad2* mutant background (A) or *UAS-dicer2/+; Mef2-Gal4/+* control (B and C). Additionally, unpaired t-tests were performed in D as indicated by lines. ###p<0.001 from unpaired t-test.

Fig. 7. Control of InR/dTOR signaling network and muscle growth by Activin signaling pathway. Activin signaling positively regulates InR/dTOR signaling by promoting the transcription of *Pdk1* and *Akt1*. Activation of InR increases PI3K-dependent PIP3 generation leading to increased activity of PDK1. PDK1 then phosphorylates AKT1 at Thr342 and S6K at Thr238. The PI3K-generated PIP3 is also necessary for activation of the dTORC2 complex which phosphorylates Ser505 of AKT1. When phosphorylated at Thr342 and Ser505 sites, AKT1 initiates a cascade of inhibition leading to activation of dTOCR1 complex that phosphorylates S6K at Thr398. The sequential phosphorylations at Thr398 and Thr238 sites fully activates S6K. The activated S6K then promotes the production of certain sarcomeric proteins as well as inhibits signal

transduction from InR to PI3K. The InR/dTORC1 signaling increases the steay-state level of MHC which is preferentially added to lateral side of existing sarcomeres when the Activin signaling is low or absent. In addition to positively regulating InR/dTOR pathway, the Activin pathway also promotes the serial assembly of sarcomeres. Mammalian homologous sites of phosphorylation are presented in parentheses.

Supplementary Figures

Fig. S1. (A) The specificity of the anti-pdSmad2 antibody was examined by immunoblot analysis. The absence of corresponding bands of pdSmad2 in *babo* and *dSmad2* mutants verifies the specificity of the antibody. The absence of pdSmad2 band in *babo* mutants also indicated that dSmad2 phosphorylation is exclusively canonical in larval body wall tissue. (B) Quantification of transcripts level of sarcomeric proteins in *wt* as well as in *babo* and *dSmad2* mutants by qPCR. Transcription of *Mhc* is not significantly altered while *Actn* expression is up-regulated by *babo* and *dSmad2* mutations. (C) Sequence alignment of myo^{CR2} mutant line with wild-type. myo^{CR2} has a lesion with one base pair deletion in the target sequence. (D) Number of nucleus from muscle 6 of abdominal segment 2 and 3. The *babo* mutant shows a similar number of nucleus as w^{1118} which we used as a wild type in this study, whereas *dSmad2* mutant exhibits an increased nucleus number compared to w^{1118} (red asterisks). When compared to *yw*, all genotypes including w^{1118} are found to have a smaller number of nucleus (black asterisks) except in the abdominal segment 3 of *dSmad2* mutant. (E) Representative immunoblot image and quantification of MHC. Co-expressed *raptorRNAi* suppressed the hyper production of MHC caused by $babo^{CA}$. (F) Quantification of transcripts level of Zasps in *wt* as well as in *babo* and *dSmad2* mutants by qPCR. Transcription of *Zasp52* is not significantly altered while *Zasp66* expression is up-regulated in *babo* and *dSmad2*

mutants. Values are mean ± SEM. *p<0.05, **p<0.01 and ***p<0.001 from one-way ANOVA followed by Dunnett's test in which each genotype was compared to *wt* (B, D and F) or *Mef2-Gal4/+* control (E). Additionally, unpaired t-tests were performed in E as indicated by lines. ##p<0.01 from unpaired t-test.

Fig. S2. Reproduction of the key results using *Mhc-Gal4* driver. (A) Representative immunoblot images of MHC and pAKT1. Overexpression of *dSmad2* transgene using *Mhc-Gal4* driver in *dSmad2* mutant background restores the altered levels of MHC and pAKT1. (B) Representative muscle images stained with Actn antibody. Overexpressing *dSmad2* transgene using *Mhc-Gal4* driver rescues the reduced size of *dSmad2* muscle. Scale bar equals 50 μm. (B') Quantification of muscle size by counting Z-discs. *Mhc-Gal4*-driven expression of *dSmad2* transgene rescues the decreased Z-disc number of *dSmad2* muscle. (C) Overexpressing *babo*^{CA} using *Mhc-Gal4* driver greatly increases the Z-disc number. Values are mean ± SEM. ###p<0.001 from unpaired t-test.

Acknowledgements

We thank Graeme W. Davis and Ernst Hafen for providing *Pdk1* mutants. We are greatful to the Bloomington *Drosophila* Stock Center for providing fly lines and Developmental Studies Hybridoma Bank for Actn antibody. We also thank Aidan Peterson, Thomas Neufeld and Hiroshi Nakato for comments on the manuscript. This work was supported by a National Institutes of Health grant (1R35 GM-118029) to M.B.O.

Fig.1 Kim and O'Connor

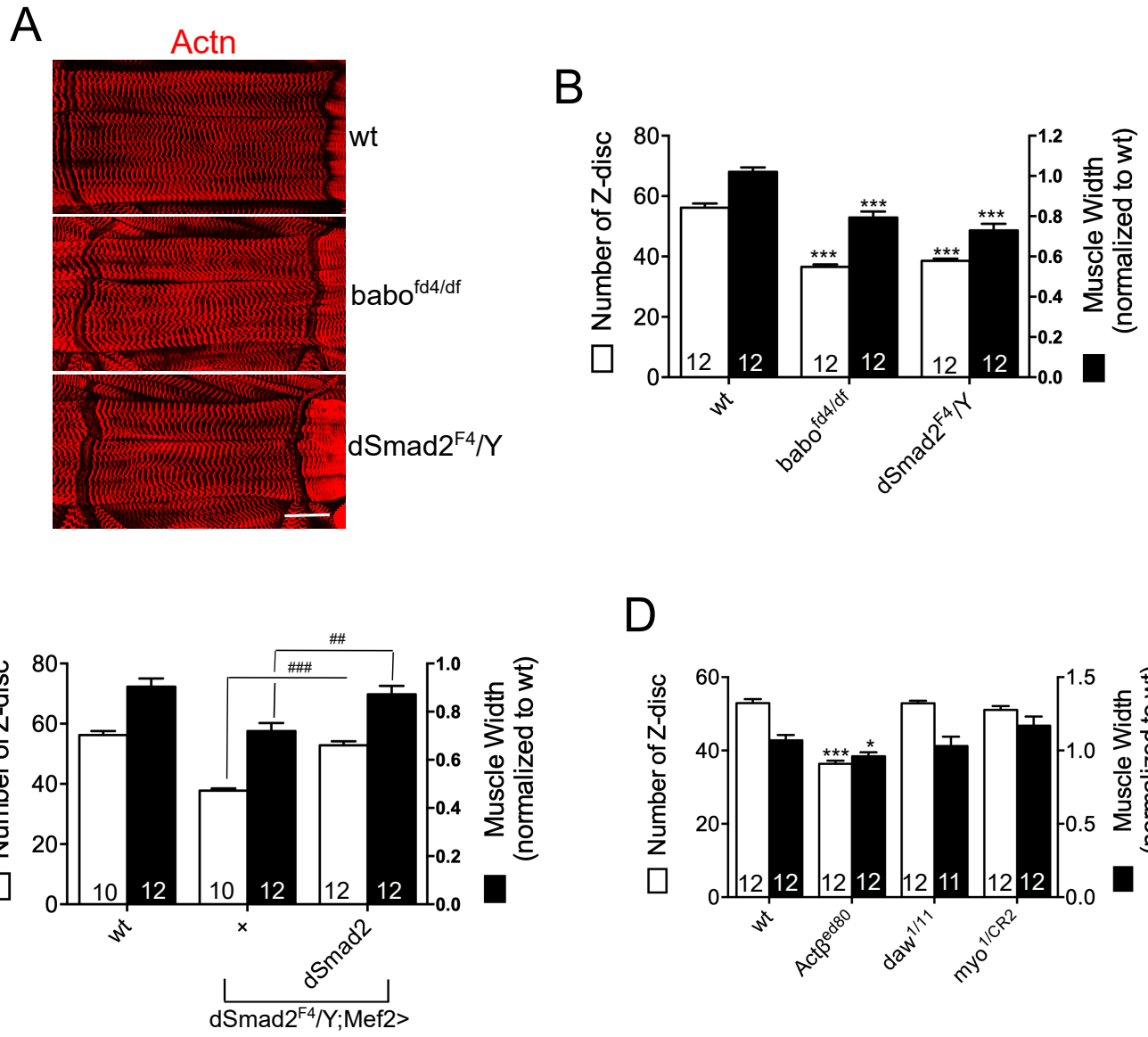

Fig.2 Kim and O'Connor

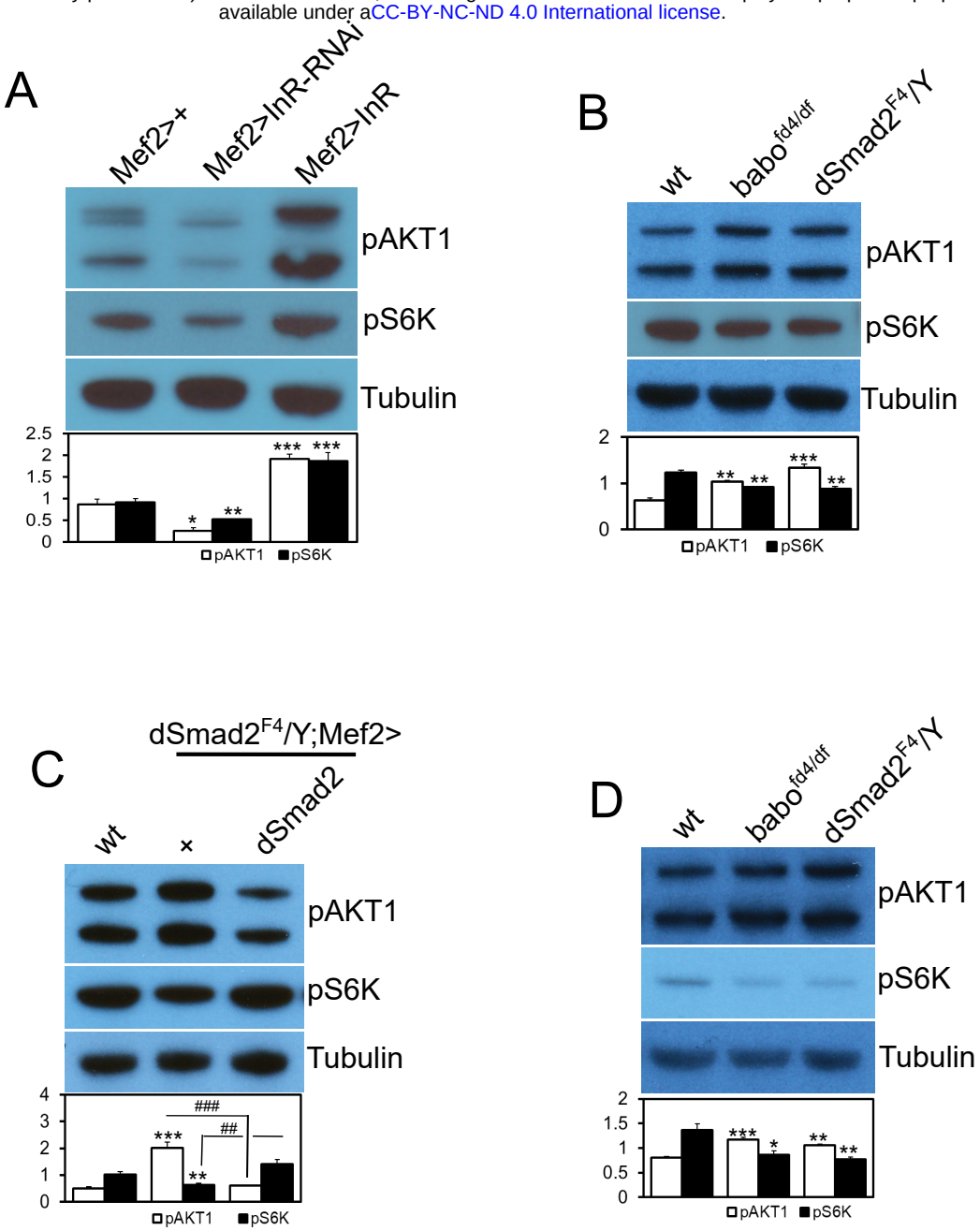

Fig.3 Kim and O'Connor

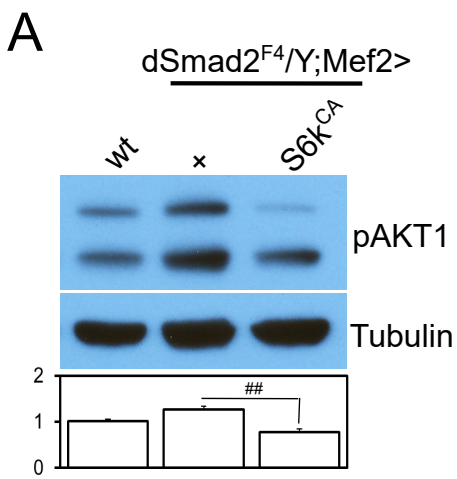

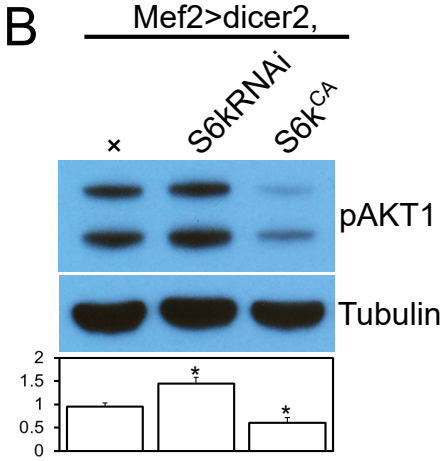

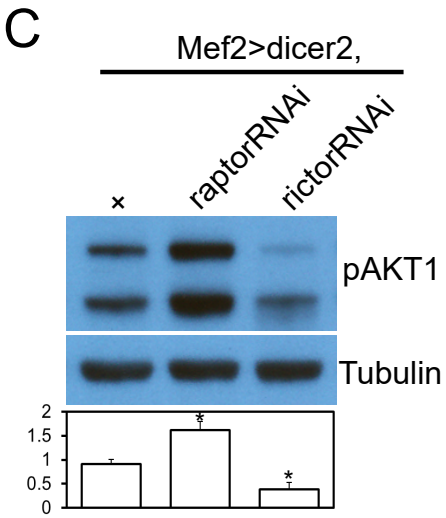

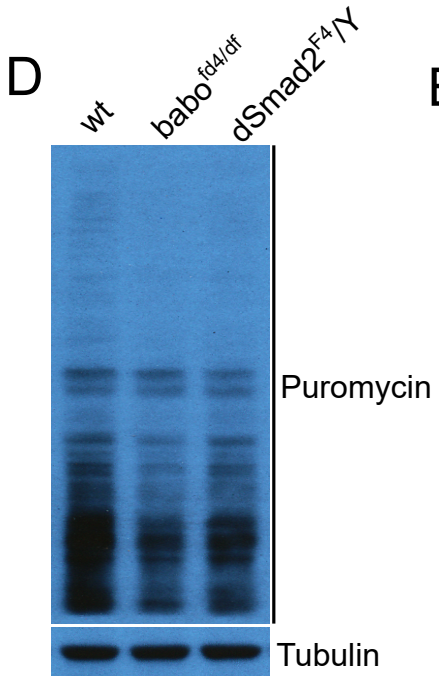

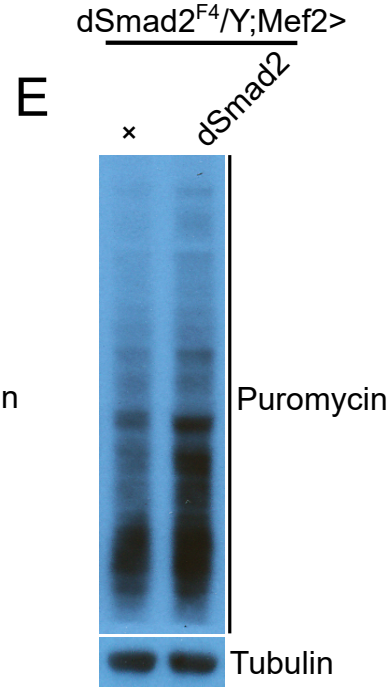

Fig.4 Kim and O'Connor

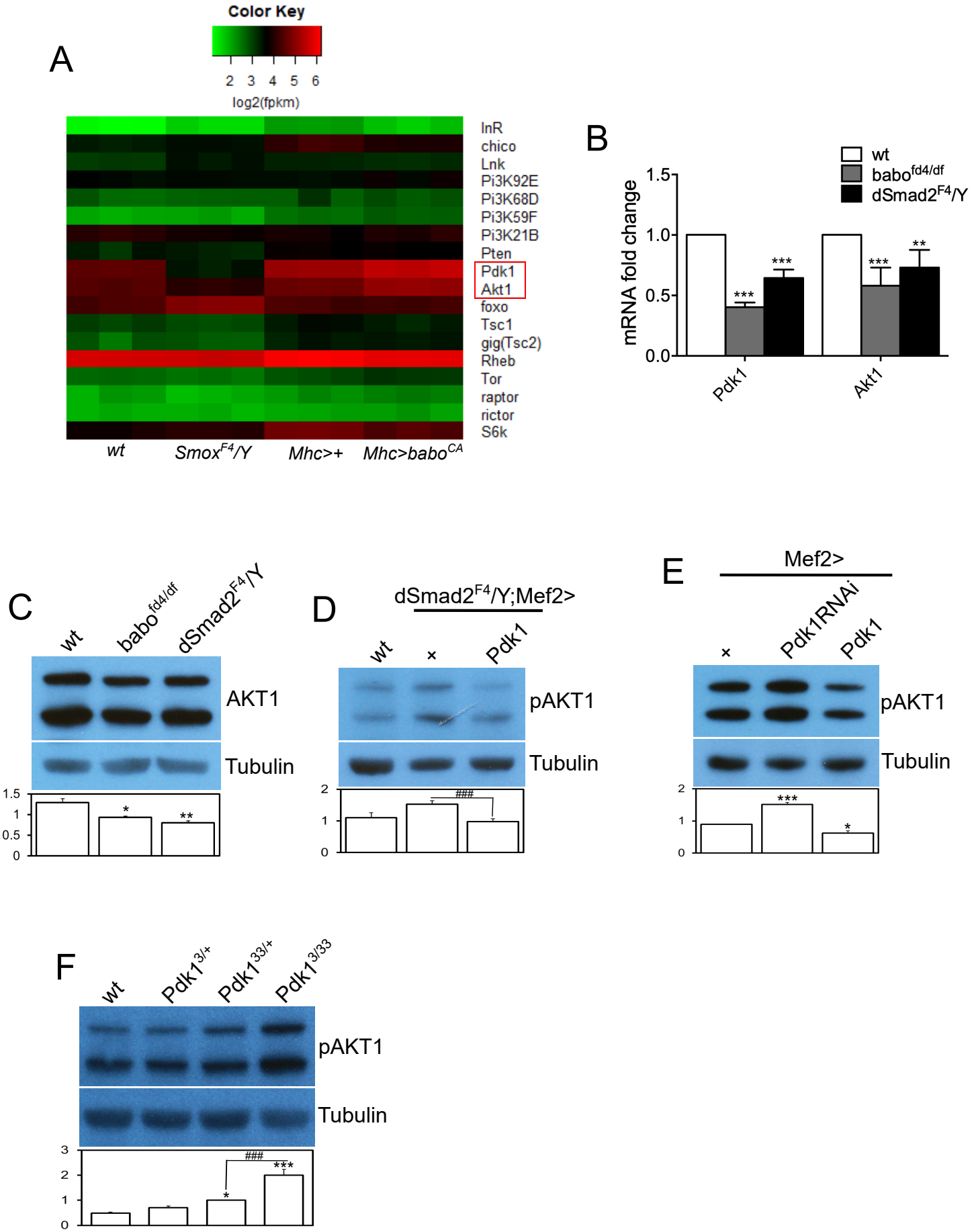

Fig.5 Kim and O'Connor

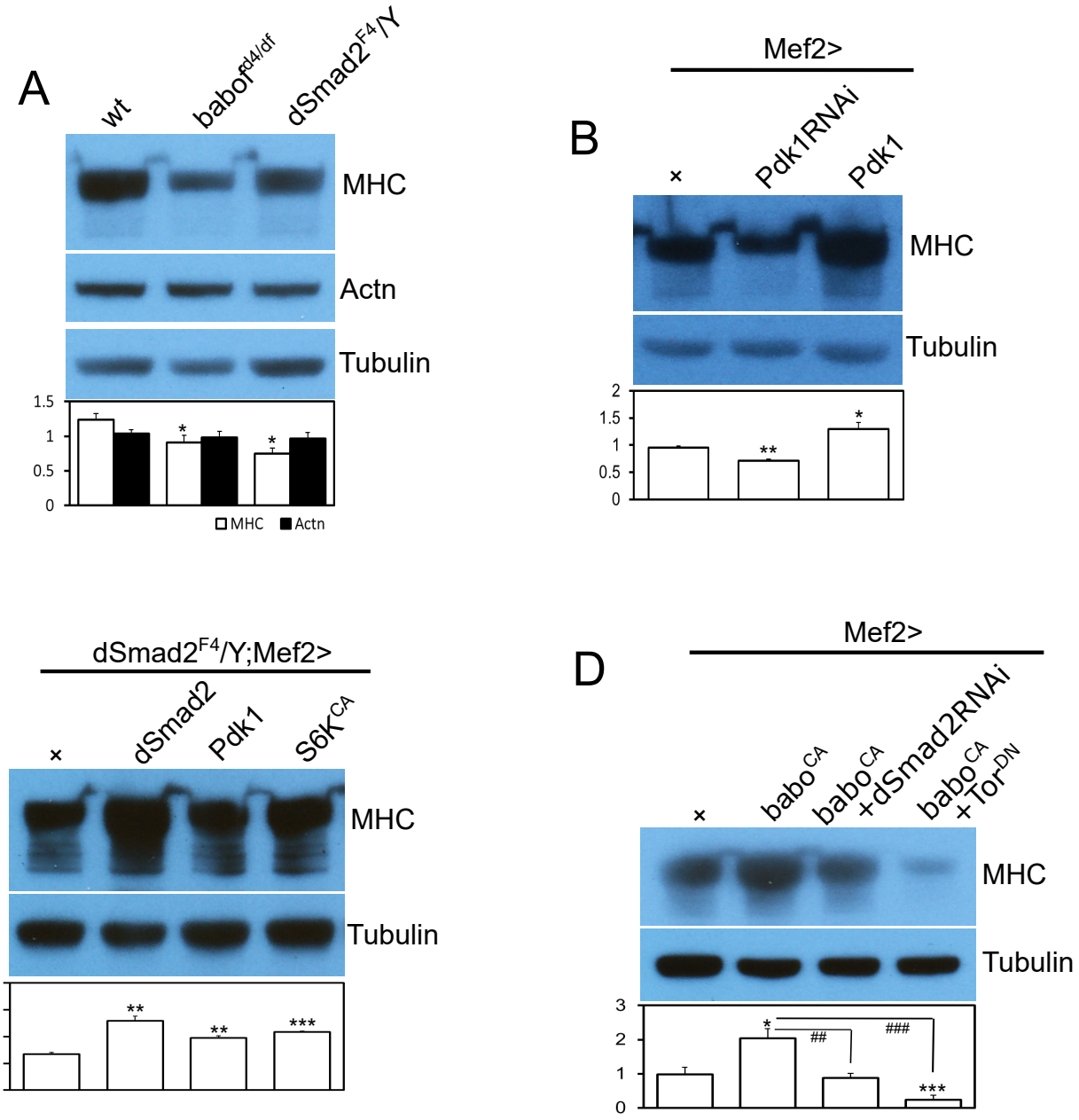

Fig.6 Kim and O'Connor

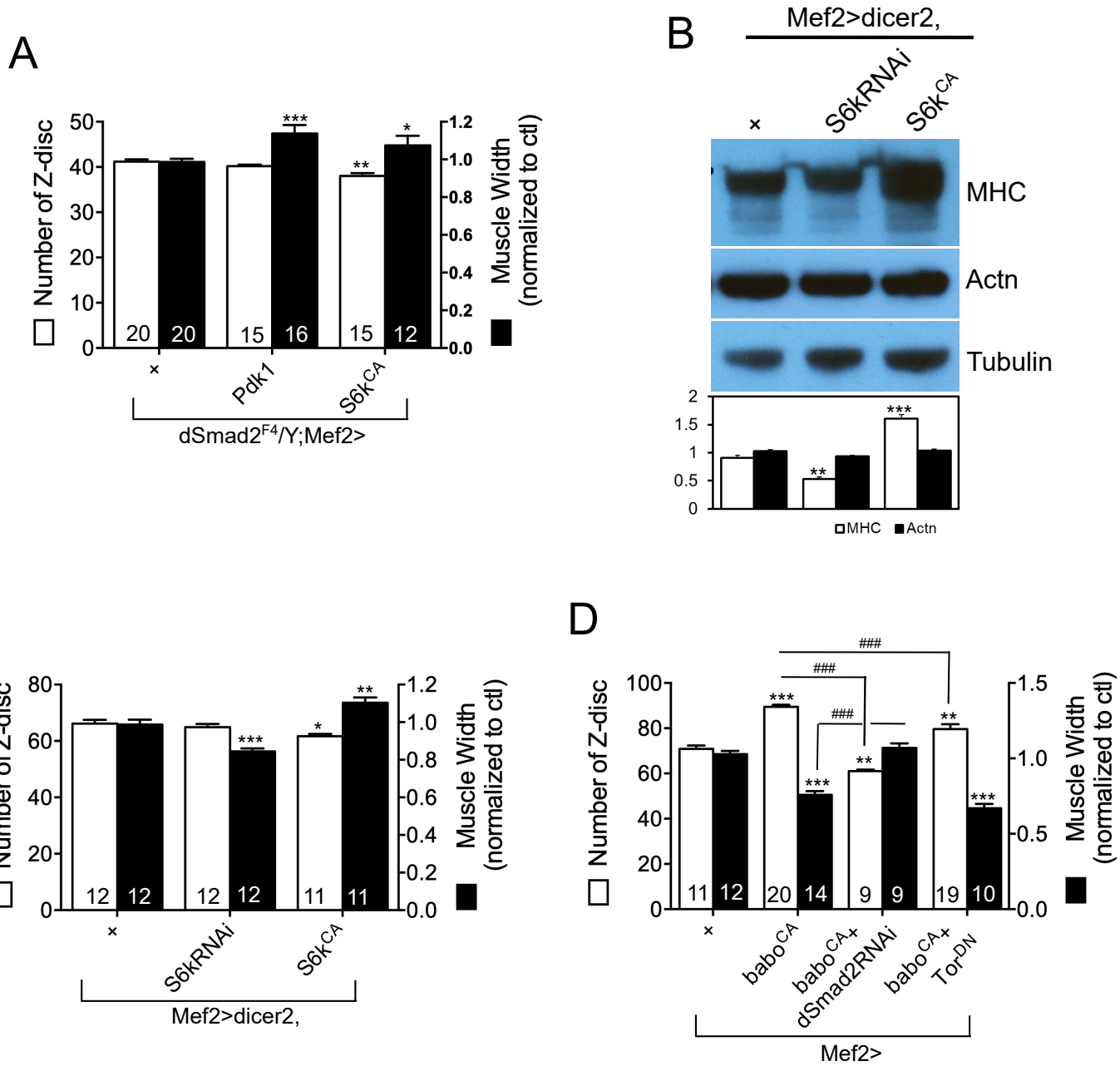

Fig.7 Kim and O'Connor

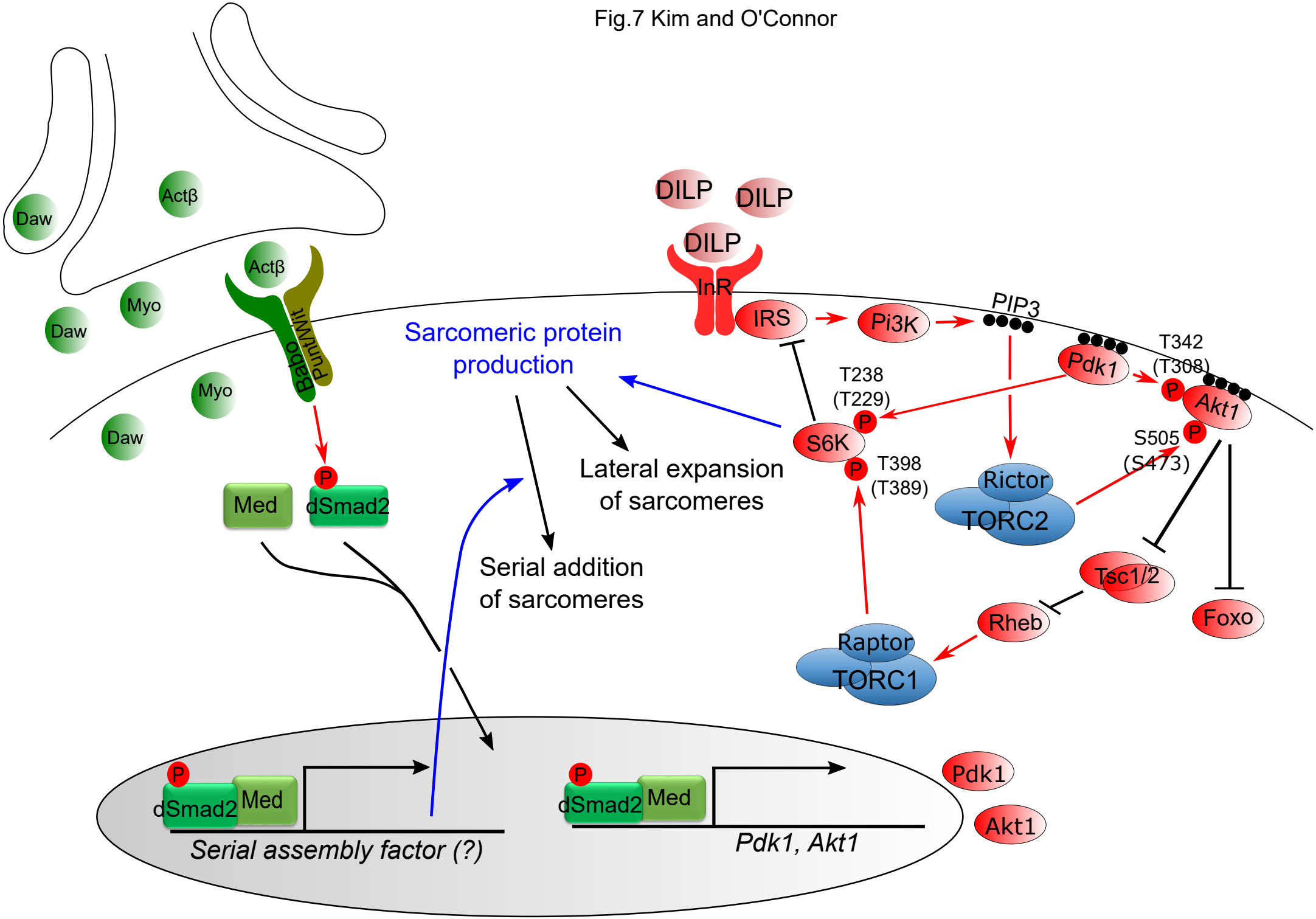

Fig. S1 Kim and O'Connor

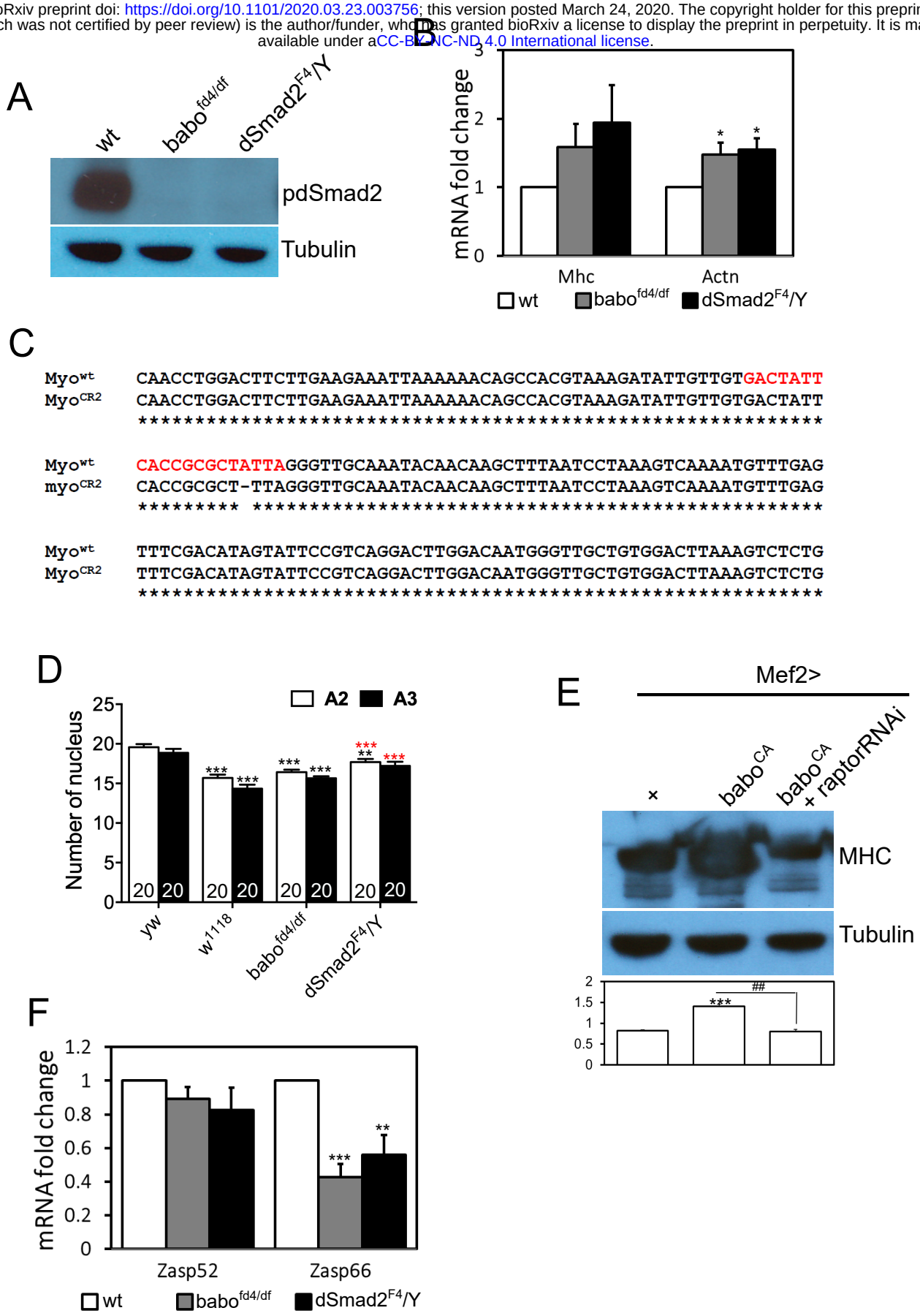

Fig. S2 Kim and O'Connor

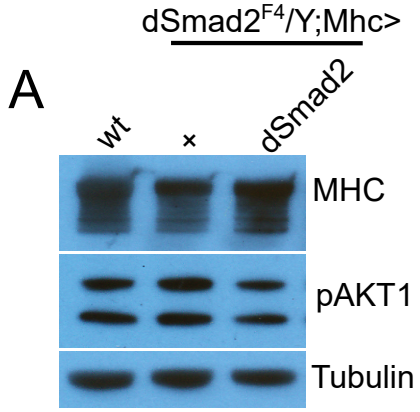

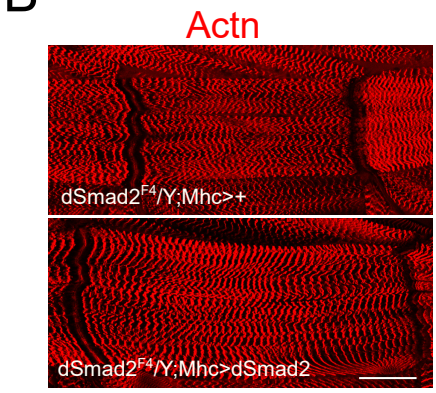

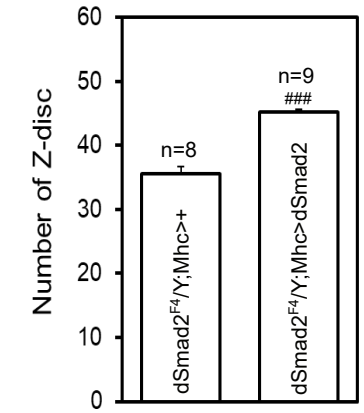

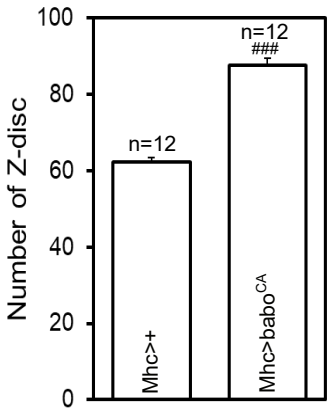

Literature Cited

Amirouche, A., Durieux, A.C., Banzet, S., Koulmann, N., Bonnefoy, R., Mouret, C., Bigard, X., Peinnequin, A., and Freyssenet, D. (2009). Down-regulation of Akt/mammalian target of rapamycin signaling pathway in response to myostatin overexpression in skeletal muscle. Endocrinology 150, 286-94.

Amthor, H., Otto, A., Vulin, A., Rochat, A., Dumonceaux, J., Garcia, L., Mouisel, E., Hourdé, C., Macharia, R., Friedrichs, M., et al. (2009). Muscle hypertrophy driven by myostatin blockade does not require stem/precursor-cell activity. Proc Natl Acad Sci U S A 106, 7479-84.

Augustin, H., McGourty, K., Steinert, J.R., Cochemé, H.M., Adcott, J., Cabecinha, M., Vincent, A., Halff, E.F., Kittler, J.T., Boucrot, E., et al. (2017). Myostatin-like proteins regulate synaptic function and neuronal morphology. Development 144, 2445-2455.

Bergen, H.R., Farr, J.N., Vanderboom, P.M., Atkinson, E.J., White, T.A., Singh, R.J., Khosla, S., and LeBrasseur, N.K. (2015). Myostatin as a mediator of sarcopenia versus homeostatic regulator of muscle mass: insights using a new mass spectrometry-based assay. Skelet Muscle 5, 21.

Bhattacharya, T.K., Shukla, R., Chatterjee, R.N., and Bhanja, S.K. (2019). Comparative analysis of silencing expression of myostatin (MSTN) and its two receptors (ACVR2A and ACVR2B) genes affecting growth traits in knock down chicken. Sci Rep 9, 7789.

Bogdanovich, S., Krag, T.O., Barton, E.R., Morris, L.D., Whittemore, L.A., Ahima, R.S., and Khurana, T.S. (2002). Functional improvement of dystrophic muscle by myostatin blockade. Nature 420, 418-21.

Bonaldo, P., and Sandri, M. (2013). Cellular and molecular mechanisms of muscle atrophy. Dis Model Mech 6, 25-39.

Brummel, T., Abdollah, S., Haerry, T.E., Shimell, M.J., Merriam, J., Raftery, L., Wrana, J.L., and O'Connor, M.B. (1999). The Drosophila activin receptor baboon signals through dSmad2 and controls cell proliferation but not patterning during larval development. Genes Dev 13, 98-111.

Chen, J.L., Walton, K.L., Al-Musawi, S.L., Kelly, E.K., Qian, H., La, M., Lu, L., Lovrecz, G., Ziemann, M., Lazarus, R., et al. (2015). Development of novel activin-targeted therapeutics. Mol Ther 23, 434-44.

Chen, J.L., Walton, K.L., Hagg, A., Colgan, T.D., Johnson, K., Qian, H., Gregorevic, P., and Harrison, C.A. (2017). Specific targeting of TGF-β family ligands demonstrates distinct roles in the regulation of muscle mass in health and disease. Proc Natl Acad Sci U S A 114, E5266-E5275.

Chen, J.L., Walton, K.L., Winbanks, C.E., Murphy, K.T., Thomson, R.E., Makanji, Y., Qian, H., Lynch, G.S., Harrison, C.A., and Gregorevic, P. (2014). Elevated expression of activins promotes muscle wasting and cachexia. FASEB J 28, 1711-23.

Cheng, L., Locke, C., and Davis, G.W. (2011). S6 kinase localizes to the presynaptic active zone and functions with PDK1 to control synapse development. J Cell Biol 194, 921-35.

Clop, A., Marcq, F., Takeda, H., Pirottin, D., Tordoir, X., Bibé, B., Bouix, J., Caiment, F., Elsen, J.M., Eychenne, F., et al. (2006). A mutation creating a potential illegitimate microRNA target site in the myostatin gene affects muscularity in sheep. Nat Genet 38, 813-8.

Das, R., Sebo, Z., Pence, L., and Dobens, L.L. (2014). Drosophila tribbles antagonizes insulin signaling-mediated growth and metabolism via interactions with Akt kinase. PLoS One 9, e109530.

De Santis, C., Wade, N.M., Jerry, D.R., Preston, N.P., Glencross, B.D., and Sellars, M.J. (2011). Growing backwards: an inverted role for the shrimp ortholog of vertebrate myostatin and GDF11. J Exp Biol 214, 2671-7.

Demontis, F., Patel, V.K., Swindell, W.R., and Perrimon, N. (2014). Intertissue control of the nucleolus via a myokine-dependent longevity pathway. Cell Rep 7, 1481-1494.

Demontis, F., and Perrimon, N. (2009). Integration of Insulin receptor/Foxo signaling and dMyc activity during muscle growth regulates body size in Drosophila. Development 136, 983-93.

Di Cara, F., and King-Jones, K. (2016). The Circadian Clock Is a Key Driver of Steroid Hormone Production in Drosophila. Curr Biol 26, 2469-2477.

Easwvaran, S.P., Bhassu, S., Maningas, M.-B.B., and Othman, R.Y. (2019). Enhanced muscle regeneration in freshwater prawn Macrobrachium rosenbergii achieved through in vivo silencing of the myostatin gene. J World Aquacult Soc 50, 1026–1039.

Eaton, B.A., and Davis, G.W. (2005). LIM Kinase1 controls synaptic stability downstream of the type II BMP receptor. Neuron 47, 695-708.

Egerman, M.A., and Glass, D.J. (2014). Signaling pathways controlling skeletal muscle mass. Crit Rev Biochem Mol Biol 49, 59-68.

El-Brolosy, M.A., Kontarakis, Z., Rossi, A., Kuenne, C., Günther, S., Fukuda, N., Kikhi, K., Boezio, G.L.M., Takacs, C.M., Lai, S.L., et al. (2019). Genetic compensation triggered by mutant mRNA degradation. Nature 568, 193-197.

El-Brolosy, M.A., and Stainier, D.Y.R. (2017). Genetic compensation: A phenomenon in search of mechanisms. PLoS Genet 13, e1006780.

Gao, Y., Dai, Z., Shi, C., Zhai, G., Jin, X., He, J., Lou, Q., and Yin, Z. (2016). Depletion of Myostatin b Promotes Somatic Growth and Lipid Metabolism in Zebrafish. Front Endocrinol (Lausanne) 7, 88.

Ghosh, A.C., and O'Connor, M.B. (2014). Systemic Activin signaling independently regulates sugar homeostasis, cellular metabolism, and pH balance in Drosophila melanogaster. Proc Natl Acad Sci U S A 111, 5729-34.

Gibbens, Y.Y., Warren, J.T., Gilbert, L.I., and O'Connor, M.B. (2011). Neuroendocrine regulation of Drosophila metamorphosis requires TGFbeta/Activin signaling. Development 138, 2693-703.

Gollnick, P.D., Timson, B.F., Moore, R.L., and Riedy, M. (1981). Muscular enlargement and number of fibers in skeletal muscles of rats. J Appl Physiol Respir Environ Exerc Physiol 50, 936-43.

González-Morales, N., Xiao, Y.S., Schilling, M.A., Marescal, O., Liao, K.A., and Schöck, F. (2019). Myofibril diameter is set by a finely tuned mechanism of protein oligomerization in. Elife 8.

Goodman, C.A., McNally, R.M., Hoffmann, F.M., and Hornberger, T.A. (2013). Smad3 induces atrogin-1, inhibits mTOR and protein synthesis, and promotes muscle atrophy in vivo. Mol Endocrinol 27, 1946-57.

Gunn, H.M. (1989). Heart weight and running ability. J Anat 167, 225-33.

Gustafsson, T., Osterlund, T., Flanagan, J.N., von Waldén, F., Trappe, T.A., Linnehan, R.M., and Tesch, P.A. (2010). Effects of 3 days unloading on molecular regulators of muscle size in humans. J Appl Physiol (1985) 109, 721-7.

Harrington, L.S., Findlay, G.M., Gray, A., Tolkacheva, T., Wigfield, S., Rebholz, H., Barnett, J., Leslie, N.R., Cheng, S., Shepherd, P.R., et al. (2004). The TSC1-2 tumor suppressor controls insulin-PI3K signaling via regulation of IRS proteins. J Cell Biol 166, 213-23.

Haun, C.T., Vann, C.G., Roberts, B.M., Vigotsky, A.D., Schoenfeld, B.J., and Roberts, M.D. (2019). A Critical Evaluation of the Biological Construct Skeletal Muscle Hypertrophy: Size Matters but So Does the Measurement. Front Physiol 10, 247.

Hietakangas, V., and Cohen, S.M. (2007). Re-evaluating AKT regulation: role of TOR complex 2 in tissue growth. Genes Dev 21, 632-7.

Hitachi, K., Nakatani, M., and Tsuchida, K. (2014). Myostatin signaling regulates Akt activity via the regulation of miR-486 expression. Int J Biochem Cell Biol 47, 93-103.

Hong, S.H., Kang, M., Lee, K.S., and Yu, K. (2016). High fat diet-induced TGF-β/Gbb signaling provokes insulin resistance through the tribbles expression. Sci Rep 6, 30265.

Hulmi, J.J., Oliveira, B.M., Silvennoinen, M., Hoogaars, W.M., Ma, H., Pierre, P., Pasternack, A., Kainulainen, H., and Ritvos, O. (2013). Muscle protein synthesis, mTORC1/MAPK/Hippo signaling, and capillary density are altered by blocking of myostatin and activins. Am J Physiol Endocrinol Metab 304, E41-50.

Kambadur, R., Sharma, M., Smith, T.P., and Bass, J.J. (1997). Mutations in myostatin (GDF8) in double-muscled Belgian Blue and Piedmontese cattle. Genome Res 7, 910-6.

Kim, M.J., and O'Connor, M.B. (2014). Anterograde Activin signaling regulates postsynaptic membrane potential and GluRIIA/B abundance at the Drosophila neuromuscular junction. PLoS One 9, e107443.

Kockel, L., Kerr, K.S., Melnick, M., Brückner, K., Hebrok, M., and Perrimon, N. (2010). Dynamic switch of negative feedback regulation in Drosophila Akt-TOR signaling. PLoS Genet 6, e1000990.

Lee, S.J., Huynh, T.V., Lee, Y.S., Sebald, S.M., Wilcox-Adelman, S.A., Iwamori, N., Lepper, C., Matzuk, M.M., and Fan, C.M. (2012). Role of satellite cells versus myofibers in muscle hypertrophy induced by inhibition of the myostatin/activin signaling pathway. Proc Natl Acad Sci U S A 109, E2353-60.

Lee, S.J., and McPherron, A.C. (2001). Regulation of myostatin activity and muscle growth. Proc Natl Acad Sci U S A 98, 9306-11.

Lee, S.J., Reed, L.A., Davies, M.V., Girgenrath, S., Goad, M.E., Tomkinson, K.N., Wright, J.F., Barker, C., Ehrmantraut, G., Holmstrom, J., et al. (2005). Regulation of muscle growth by multiple ligands signaling through activin type II receptors. Proc Natl Acad Sci U S A 102, 18117-22.

Lindquist, R.A., Ottina, K.A., Wheeler, D.B., Hsu, P.P., Thoreen, C.C., Guertin, D.A., Ali, S.M., Sengupta, S., Shaul, Y.D., Lamprecht, M.R., et al. (2011). Genome-scale RNAi on living-cell microarrays identifies novel regulators of Drosophila melanogaster TORC1-S6K pathway signaling. Genome Res 21, 433-46.

Lokireddy, S., Mouly, V., Butler-Browne, G., Gluckman, P.D., Sharma, M., Kambadur, R., and McFarlane, C. (2011). Myostatin promotes the wasting of human myoblast cultures through promoting ubiquitin-proteasome pathway-mediated loss of sarcomeric proteins. Am J Physiol Cell Physiol 301, C1316-24.

Lokireddy, S., Wijesoma, I.W., Bonala, S., Wei, M., Sze, S.K., McFarlane, C., Kambadur, R., and Sharma, M. (2012). Myostatin is a novel tumoral factor that induces cancer cachexia. Biochem J 446, 23-36.

Loumaye, A., de Barsy, M., Nachit, M., Lause, P., Frateur, L., van Maanen, A., Trefois, P., Gruson, D., and Thissen, J.P. (2015). Role of Activin A and myostatin in human cancer cachexia. J Clin Endocrinol Metab 100, 2030-8.

Marden, J.H. (2000). Variability in the size, composition, and function of insect flight muscles. Annu Rev Physiol 62, 157-78.

Marino, F.E., Risbridger, G., and Gold, E. (2015). Activin-βC modulates cachexia by repressing the ubiquitin-proteasome and autophagic degradation pathways. J Cachexia Sarcopenia Muscle 6, 365-80.

McCabe, B.D., Marqués, G., Haghighi, A.P., Fetter, R.D., Crotty, M.L., Haerry, T.E., Goodman, C.S., and O'Connor, M.B. (2003). The BMP homolog Gbb provides a retrograde signal that regulates synaptic growth at the Drosophila neuromuscular junction. Neuron 39, 241-54.

McFarland, D.C., Velleman, S.G., Pesall, J.E., and Liu, C. (2006). Effect of myostatin on turkey myogenic satellite cells and embryonic myoblasts. Comp Biochem Physiol A Mol Integr Physiol 144, 501-8.

McPherron, A.C., Lawler, A.M., and Lee, S.J. (1997). Regulation of skeletal muscle mass in mice by a new TGF-beta superfamily member. Nature 387, 83-90.

McPherron, A.C., and Lee, S.J. (1997). Double muscling in cattle due to mutations in the myostatin gene. Proc Natl Acad Sci U S A 94, 12457-61.

Mosher, D.S., Quignon, P., Bustamante, C.D., Sutter, N.B., Mellersh, C.S., Parker, H.G., and Ostrander, E.A. (2007). A mutation in the myostatin gene increases muscle mass and enhances racing performance in heterozygote dogs. PLoS Genet 3, e79.

Moss-Taylor, L., Upadhyay, A., Pan, X., Kim, M.J., and O'Connor, M.B. (2019). Body Size and Tissue-Scaling Is Regulated by Motoneuron-Derived Activinß in. Genetics 213, 1447-1464.

Ng, J. (2008). TGF-beta signals regulate axonal development through distinct Smad-independent mechanisms. Development 135, 4025-35.

Parker, L., Stathakis, D.G., and Arora, K. (2004). Regulation of BMP and activin signaling in Drosophila. Prog Mol Subcell Biol 34, 73-101.

Paul, A.C., and Rosenthal, N. (2002). Different modes of hypertrophy in skeletal muscle fibers. J Cell Biol 156, 751-60.

Pedersen, B.K., and Febbraio, M.A. (2012). Muscles, exercise and obesity: skeletal muscle as a secretory organ. Nat Rev Endocrinol 8, 457-65.

Piccirillo, R., Demontis, F., Perrimon, N., and Goldberg, A.L. (2014). Mechanisms of muscle growth and atrophy in mammals and Drosophila. Dev Dyn 243, 201-15.

Pullen, N., Dennis, P.B., Andjelkovic, M., Dufner, A., Kozma, S.C., Hemmings, B.A., and Thomas, G. (1998). Phosphorylation and activation of p70s6k by PDK1. Science 279, 707-10.

Reardon, K.A., Davis, J., Kapsa, R.M., Choong, P., and Byrne, E. (2001). Myostatin, insulin-like growth factor-1, and leukemia inhibitory factor mRNAs are upregulated in chronic human disuse muscle atrophy. Muscle Nerve 24, 893-9.

Rintelen, F., Stocker, H., Thomas, G., and Hafen, E. (2001). PDK1 regulates growth through Akt and S6K in Drosophila. Proc Natl Acad Sci U S A 98, 15020-5.

Rosenblatt, J.D., and Woods, R.I. (1992). Hypertrophy of rat extensor digitorum longus muscle injected with bupivacaine. A sequential histochemical, immunohistochemical, histological and morphometric study. J Anat 181 (Pt 1), 11-27.

Sarbassov, D.D., Guertin, D.A., Ali, S.M., and Sabatini, D.M. (2005). Phosphorylation and regulation of Akt/PKB by the rictor-mTOR complex. Science 307, 1098-101.

Sartori, R., Gregorevic, P., and Sandri, M. (2014). TGFβ and BMP signaling in skeletal muscle: potential significance for muscle-related disease. Trends Endocrinol Metab 25, 464-71.

Sartori, R., Milan, G., Patron, M., Mammucari, C., Blaauw, B., Abraham, R., and Sandri, M. (2009). Smad2 and 3 transcription factors control muscle mass in adulthood. Am J Physiol Cell Physiol 296, C1248-57.

Sartori, R., Schirwis, E., Blaauw, B., Bortolanza, S., Zhao, J., Enzo, E., Stantzou, A., Mouisel, E., Toniolo, L., Ferry, A., et al. (2013). BMP signaling controls muscle mass. Nat Genet 45, 1309-18.

Schiaffino, S., Dyar, K.A., Ciciliot, S., Blaauw, B., and Sandri, M. (2013). Mechanisms regulating skeletal muscle growth and atrophy. FEBS J 280, 4294-314.

Schiaffino, S., and Mammucari, C. (2011). Regulation of skeletal muscle growth by the IGF1-Akt/PKB pathway: insights from genetic models. Skelet Muscle 1, 4.

Schmidt, E.K., Clavarino, G., Ceppi, M., and Pierre, P. (2009). SUnSET, a nonradioactive method to monitor protein synthesis. Nat Methods 6, 275-7.

Schuelke, M., Wagner, K.R., Stolz, L.E., Hübner, C., Riebel, T., Kömen, W., Braun, T., Tobin, J.F., and Lee, S.J. (2004). Myostatin mutation associated with gross muscle hypertrophy in a child. N Engl J Med 350, 2682-8.

Shah, O.J., Wang, Z., and Hunter, T. (2004). Inappropriate activation of the TSC/Rheb/mTOR/S6K cassette induces IRS1/2 depletion, insulin resistance, and cell survival deficiencies. Curr Biol 14, 1650-6.

Souza, T.A., Chen, X., Guo, Y., Sava, P., Zhang, J., Hill, J.J., Yaworsky, P.J., and Qiu, Y. (2008). Proteomic identification and functional validation of activins and bone morphogenetic protein 11 as candidate novel muscle mass regulators. Mol Endocrinol 22, 2689-702.

Stantzou, A., Schirwis, E., Swist, S., Alonso-Martin, S., Polydorou, I., Zarrouki, F., Mouisel, E., Beley, C., Julien, A., Le Grand, F., et al. (2017). BMP signaling regulates satellite cell-dependent postnatal muscle growth. Development 144, 2737-2747.

Stump, C.S., Henriksen, E.J., Wei, Y., and Sowers, J.R. (2006). The metabolic syndrome: role of skeletal muscle metabolism. Ann Med 38, 389-402.

Tan, C.K., Leuenberger, N., Tan, M.J., Yan, Y.W., Chen, Y., Kambadur, R., Wahli, W., and Tan, N.S. (2011). Smad3 deficiency in mice protects against insulin resistance and obesity induced by a high-fat diet. Diabetes 60, 464-76.

Tando, T., Hirayama, A., Furukawa, M., Sato, Y., Kobayashi, T., Funayama, A., Kanaji, A., Hao, W., Watanabe, R., Morita, M., et al. (2016). Smad2/3 Proteins Are Required for Immobilization-induced Skeletal Muscle Atrophy. J Biol Chem 291, 12184-94.

Timson, B.F., and Dudenhoeffer, G.A. (1990). Skeletal muscle fibre number in the rat from youth to adulthood. J Anat 173, 33-6.

Ting, C.Y., Herman, T., Yonekura, S., Gao, S., Wang, J., Serpe, M., O'Connor, M.B., Zipursky, S.L., and Lee, C.H. (2007). Tiling of r7 axons in the Drosophila visual system is mediated both by transduction of an activin signal to the nucleus and by mutual repulsion. Neuron 56, 793-806.

Trendelenburg, A.U., Meyer, A., Rohner, D., Boyle, J., Hatakeyama, S., and Glass, D.J. (2009). Myostatin reduces Akt/TORC1/p70S6K signaling, inhibiting myoblast differentiation and myotube size. Am J Physiol Cell Physiol 296, C1258-70.

Um, S.H., Frigerio, F., Watanabe, M., Picard, F., Joaquin, M., Sticker, M., Fumagalli, S., Allegrini, P.R., Kozma, S.C., Auwerx, J., et al. (2004). Absence of S6K1 protects against age- and diet-induced obesity while enhancing insulin sensitivity. Nature 431, 200-5.

Upadhyay, A., Moss-Taylor, L., Kim, M.J., Ghosh, A.C., and O'Connor, M.B. (2017). TGF-β Family Signaling in. Cold Spring Harb Perspect Biol 9.

Watanabe, H., Schmidt, H.A., Kuhn, A., Höger, S.K., Kocagöz, Y., Laumann-Lipp, N., Ozbek, S., and Holstein, T.W. (2014). Nodal signalling determines biradial asymmetry in Hydra. Nature 515, 112-5.

Wehling, M., Cai, B., and Tidball, J.G. (2000). Modulation of myostatin expression during modified muscle use. FASEB J 14, 103-10.

White, T.A., and LeBrasseur, N.K. (2014). Myostatin and sarcopenia: opportunities and challenges - a mini-review. Gerontology 60, 289-93.

Winbanks, C.E., Chen, J.L., Qian, H., Liu, Y., Bernardo, B.C., Beyer, C., Watt, K.I., Thomson, R.E., Connor, T., Turner, B.J., et al. (2013). The bone morphogenetic protein axis is a positive regulator of skeletal muscle mass. J Cell Biol 203, 345-57.

Winbanks, C.E., Weeks, K.L., Thomson, R.E., Sepulveda, P.V., Beyer, C., Qian, H., Chen, J.L., Allen, J.M., Lancaster, G.I., Febbraio, M.A., et al. (2012). Follistatin-mediated skeletal muscle hypertrophy is regulated by Smad3 and mTOR independently of myostatin. J Cell Biol 197, 997-1008.

Yang, Q., Inoki, K., Kim, E., and Guan, K.L. (2006). TSC1/TSC2 and Rheb have different effects on TORC1 and TORC2 activity. Proc Natl Acad Sci U S A 103, 6811-6.

Zhang, J., Gao, Z., Yin, J., Quon, M.J., and Ye, J. (2008). S6K directly phosphorylates IRS-1 on Ser-270 to promote insulin resistance in response to TNF-(alpha) signaling through IKK2. J Biol Chem 283, 35375-82.

Zhang, Y.E. (2009). Non-Smad pathways in TGF-beta signaling. Cell Res 19, 128-39.

Zhou, X., Wang, J.L., Lu, J., Song, Y., Kwak, K.S., Jiao, Q., Rosenfeld, R., Chen, Q., Boone, T., Simonet, W.S., et al. (2010). Reversal of cancer cachexia and muscle wasting by ActRIIB antagonism leads to prolonged survival. Cell 142, 531-43.

Zimmers, T.A., Davies, M.V., Koniaris, L.G., Haynes, P., Esquela, A.F., Tomkinson, K.N., McPherron, A.C., Wolfman, N.M., and Lee, S.J. (2002). Induction of cachexia in mice by systemically administered myostatin. Science 296, 1486-8.